AN IMPROVED METHOD FOR ELIMINATING STRESS CONCENTRATION IN A FINITE ELEMENT MODEL

By

Rizwan Ahmed

2010-NUST-MS PHD-Mech-26

MS-64 (ME)

Submitted to the Department of Mechanical Engineering in fulfillment of the requirements for the degree of

MASTER OF SCIENCE

in

MECHANICAL ENGINEERING

Thesis Supervisor

Dr. Hasan Aftab Saeed

College of Electrical & Mechanical Engineering
National University of Sciences & Technology
2014

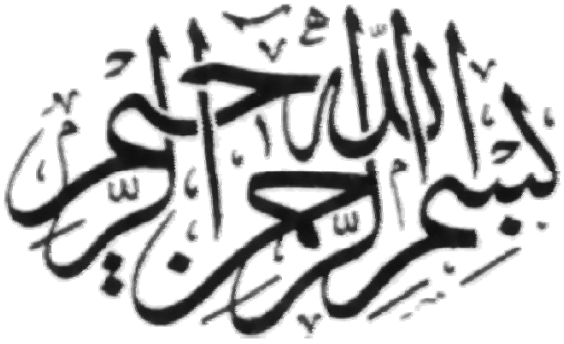

In The Name Of Allah,

The Most Beneficent

And

The Most Merciful

CERTIFICATE OF COMPLETENESS

It is hereby certified that the dissertation submitted by NS Rizwan Ahmed, Reg No. 2010-NUST-MS-PhD-Mech-26, titled: "An improved method for eliminating stress concentration in a FE model" has been checked/reviewed and its contents are complete in all respects.

Supervisor's Name: Dr. Hasan Aftab Saeed

Signature: _____

Date: _____

Table of Contents

List of Figures

List of Tables

List of Charts

ABSTRACT

The reliability of a mechanical design is established by design validation that is carried out using finite element method. Such a numerical technique method provides a very useful alternative to experimental testing which can be very expensive. During FE analysis, the overestimated stress concentrations need to be resolved or in some cases eliminated, in order to predict the actual response of the material. This thesis is aimed at developing a new and improved method for resolving and eliminating overestimated stress concentrations from an FE model. The proposed method is validated using an appropriate geometry whose experimental results are available. This will result in a provision aimed at better mechanical design methodology for application on any finite element static analysis.

DECLARATION

I hereby declare that I have developed this thesis entirely on the basis of my personal efforts under the sincere guidance of my supervisor Dr.Hasan Aftab Saeed and Dr. Abdul Rauf. All the sources used in this thesis have been cited and the contents of this thesis have not been plagiarized. No portion of the work presented in this thesis has been submitted in support of any application for any other degree of qualification to this or any other university or institute of learning.

_____

Rizwan Ahmed

Dedicated to my parents, siblings, wife and my adorable daughter

ACKNOWLEDGEMENTS

First of all, I am grateful to **Allah Almighty**, “The Lord Of The Worlds”, for establishing me to complete this thesis.

I would like to thank my graduate advisors Dr. Hasan Aftab Saeed and Dr. Abdul Rauf for their excellent support and guidance. Their constant encouragement and motivation has helped me towards successful completion of my thesis.

I would like to express my gratitude to Dr. Aamir Ahmed Baqai and Dr. Rizwan Saeed Choudhry for being the part of Guidance and Examination Committee members and their valuable suggestions and comments were a great source to improve the research work presented in this thesis.

I thank all my friends and colleagues who helped me during my thesis work.

I am extremely grateful to my family for their unconditional love, encouragement and constant support throughout my academic career.

1 INTRODUCTION

1.1 Introduction

The ultimate goal of mechanical design process is to keep the maximum stresses that are caused by loads, below the yield stress limit of the material. On contrary, faulty mechanical designs often lead to catastrophic consequences.

One of the critical aspect in mechanical design is the presence of stress concentrations. The discontinuities in the geometry result in a localized amplification of stress in some regions. Mostly these stress concentrations occur at sharp corners, holes, notch tips etc. For an efficient mechanical design, it should be known exactly how much the stress is amplified at these points. Stress concentration factors give us an idea of how many times higher is the stress going to be because of the presence of these geometric discontinuities.

Mechanical design processes are getting reshaped as mechanical structures are being designed and manufactured with improved strength and smarter measurements in order to fulfill their objectives efficiently. Numerical simulations are the first choice for any new conceptual design assessment. This is followed by experimental testing, which is comparatively much more expensive. Finite Element Analysis (FEA) makes use of this method known as finite element method (FEM) which relies on dividing the geometry into small discrete regions known as elements and subsequently solution can be attained for each node on those elements. However, this approximate FEM solution results in divergence from realistic scenarios [5].

Common errors encountered in FEA include *idealization errors* as mathematical model is derived from the simplification of reality, *discretization errors* when a continuum is replaced with a set of discrete regions (meshing), *numerical errors* introduced by the solution of the discrete system and *interpretation errors* as the results are analyzed. Therefore there are some limitations to these numerical solutions and these concerns must be tackled for a more precise solution.

One of the drawbacks in finite element analysis is occurrence of overestimated and exaggerated stress concentrations at localized regions. This strange and unexpected trend is due to the finite element methods and modeling practices instead of stress concentrations that exist because of geometric non linearities. Thus, it has been seen that at times the maximum stress observed in

linear finite element analysis do not represent the actual state of affairs. Especially for notches with small radii, up to 10% overestimation is observed when FEA stress concentration factor is compared with empirical/experimental stress concentration factor. The overestimation of stress concentration in finite element model can be most likely due to inadequate mesh density or unreasonable nodal connectivity. This results in the limitation of design with respect to its performance.

1.2 Aim of Study

The aim of this research is to investigate, develop and validate a new and improved method to resolve and eliminate unreal and exaggerated stress concentrations from an FE model within the linear elastic region. The validation will be carried out by comparing FEA results with the available empirical solutions/experimental results. Three cases will be dealt with for the sake of repeatability:

- Case 1 : Opposite single U-notch in finite width plate (P=40N)
- Case 2 : Opposite single V-notch in finite width plate (P=40N)
- Case 3: Opposite single V-notch in finite width plate (P=100N)

1.3 Methodology

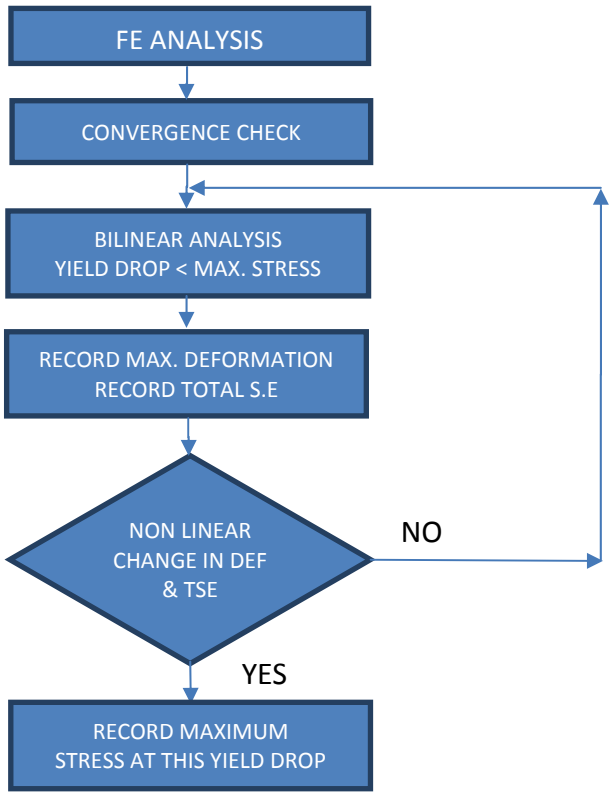

Figure 1: Methodology

1.4 Proposal

In the proposed methodology, a bi linear analysis is carried out in which the material's yield stress is initially specified less than the maximum concentrated stress in the finite element analysis (FEA) and then decreased successively. The continual decrease in yield stress of the material results in material flow within that localized region and uniform distribution of maximum stress will take place in the vicinity of that stress concentration region. Maximum stress level will reduce but with an increase in overall deformation and increased total strain energy in the structure. This overall deformation and total strain energy may be somewhat overestimated when matched with empirical values, but maximum stress value will be reduced. In our research we will observe how yielding influences the deflection as well as the total strain energy and the amount of stress resolved for different geometries and different loading scenarios. Finally, a tolerable level of yield drop will be established to prevent any unrealistic change in deflection and unrealistic change in total strain energy.

1.5 Scope of Study

The objective of this research is to investigate, develop and validate a new method to resolve and eliminate the unreal overestimated stress concentration in FE model. The stress levels will be studied within the linear elastic range. Stress concentration factor and the maximum stress value for the specified geometry will be calculated by empirical solutions/experimental results. The same geometry will be modeled using ANSYS and linear FEA will be performed first to determine the maximum stress encountered in the system. Stress concentration factor and maximum stress value determined by the FE analysis will be compared to the stress concentration factor and maximum stress value calculated by formula earlier. Unreal and exaggerated stress concentrations will be then resolved and eliminated by carrying out a bi-linear analysis. Results will be analyzed after artificially introducing a non-linear material model and forced yielding. The corresponding changes in the overall deformation and total strain energy will be studied.

2 LITERATURE REVIEW

Several studies [1-3] have been carried out to improve the structural design by removing geometric stress concentration. However removing the unreal overestimated stress concentrations encountered in finite element model by this methodology has not been published. Overestimation of stress concentration in finite element model may be more likely due to inadequate mesh density or unreasonable nodal connectivity. It has also been observed that mesh density as well as meshing method, considerably influences the FEA results.

M. Murat Topac, H. Eren Enginar, N. Sefa Kuralay [1] assessed the effect of two design parameters i.e. the transition length and transition radius of the critical region's geometry on the stress concentration at the corner bends of an anti-roll bar with the help of Design of Experiments approach. Finite element analysis was used to obtain maximum stress values in order to determine different design possibilities.

David Taylor, Andrew Kelly, Matteo Toso and Luca Susmel [2] presented two approaches for attaining variable-radius notches. The first approach known as Local Curvature Method (LCM) is implemented by initially performing a stress analysis on a constant radius notch and then using the post processing results to change the local curvature as a function of local surface stresses. LCM was observed to successfully reduce maximum stress at a 90^{o} fillet by factor of 2. In their second approach, a commercial software (modeFrontier) was used to investigate the possibility of different variable radius notch designs with the help of different finite element models. The results were seen to be better in spite of being expensive as far as computing resources were concerned. Verification was done by carrying out experimental tests to measure brittle fracture strength.

Monika G. Garrell, Albert J. Shih, Edgar Lara-Curzio, and Ronald O. Scattergood [3] investigated the stress concentrations at specific locations in ASTM D 638 Type IV flat tension specimen with the help of experimental results and finite element analysis. They established a linear relationship between the magnitude of the stress concentration factor and the ratio of the width in the gage section and the arc radius of the transition region. Their study indicated that the magnitude of the stress concentration factor can be reduced by redesigning the specimen

geometry without changing its overall size particularly by increasing the radius of the arc in the transitional area.

My research involves resolving and eliminating overestimated, unreal and exaggerated stress concentration in a finite element model without changing the geometry of the structure. The size and dimensions of the structure remain unchanged from the beginning till the point where the stress concentration is resolved by this method. With no change being done in the geometry, the application of this technique will ensure an improved structural design with low computational costs.

3 STRESS CONCENTRATION

3.1 Stress Concentrations

A localized intensification of a stress field due to geometric discontinuities in an object is called a stress concentration. The region where the geometry rapidly changes upsets the smooth flow of stresses. These stress concentrations mostly occur at sharp corners, holes and notch tips. For an efficient mechanical design, it is vital to know exactly how much the stress is amplified at these points. Stress concentration factor K_t gives us this measure of how much the maximum stress will exceed the nominal values of stress. Stress concentration factor is calculated by the following formula

Stress concentration factor $Kt = \frac{\sigma_{MAX}}{\sigma_{NOM}}$ for normal stress (tension or bending)

The maximum stress produced in the structure is evaluated on the basis of the elasticity theory and it can be obtained from an experiment or by finite element analysis. According to the theory of elasticity, for a homogeneous elastic body, 2D distribution of stress under known loading is a function of only geometry and does not depend on the material properties.

Since the ultimate goal of the mechanical design is to keep the maximum stresses that are caused by loads below the yield stress limit of the material, we are going to deal with elastic stress concentration factors throughout our study.

3.2 Accurateness of stress concentration factor

Stress concentration factors are attained with the help of elasticity theory in the form of analytical solutions, with finite element method in the form of computational results, and with photo elastic and strain gage tests in the form of experimental results. When the experimental testing is carried out with adequate accuracy, close agreement is expected to be achieved with well-recognized analytical stress concentration factors. The theoretical base for determining the stress concentration factors is more solid than the use of these factors for design and analysis. The solutions for the theory of elasticity are established on formulations that assume the material to be isotropic and homogenous. On the other hand, in reality materials may be neither uniform nor homogenous and may even contain defects. For the accuracy that is wanted, statistical routines need to be carried out and so more data is often demanded. At the same time, directional effects present in materials should be cautiously considered. The mechanical design engineer may not delay his work to search for precise answers to these questions. Therefore the available

information must be reviewed each time while the conclusions should be made use in outlining reliable approximate design procedures and inclining to a safe side in case of doubtful scenarios.

3.3 Stress concentration (2D scenario)

For a thin plate that is subjected to forces applied at the boundary in the x-y plane, the stress components σz, τxz τyz are assumed to be zero. This is called plane stress state and the stress components σx, σy, τxy are functions of x and y only.

In a plane elastic body, the equilibrium equations along with the compatibility equation for the stresses σx, σy, τxy are

$$\frac{\partial \sigma x}{\partial x} + \frac{\partial \tau xy}{\partial x} + \acute{P}Vx = 0$$

$$\frac{\partial \tau xy}{\partial x} + \frac{\partial \sigma y}{\partial y} + \acute{P}Vy = 0$$

$$\left(\frac{\partial^2}{\partial x^2} + \frac{\partial^2}{\partial y^2}\right)(\sigma x + \sigma y) = -f(v)\left(\frac{\partial \acute{P}Vx}{\partial x} + \frac{\partial \acute{P}Vy}{\partial y}\right)$$

Where $\acute{P}Vx$, $\acute{P}Vy$ represent the body force/unit volume components in x and y directions and f(v) is a function of Poisson's ratio where f(v) = 1+v for plane stress.

The surface conditions are

$$p_x = l\sigma_x + m\tau_{xy}$$

$$p_y = l\tau_{xy} + m\sigma_y$$

Where px, py are the surface force / unit area components at the boundary in the x and y directions. l and m are the direction cosines of the normal to the boundary. For constant body forces $\frac{\partial \acute{P}Vx}{\partial x} = \frac{\partial \acute{P}Vy}{\partial y} = 0$ and the equation becomes

$$\left(\frac{\partial^2}{\partial x^2} + \frac{\partial^2}{\partial y^2}\right)(\sigma x + \sigma y) = 0$$

For 2D problems with constant body forces, usually these equations are enough to evaluate the distribution of stress. However, these equations do not consist of material constants. Therefore in case of plane problems with constant body forces, the stress distribution depends on the

geometry and loadings on the boundary and does not depend on the material. Similarly this means that for plane problems, stress concentration factors are functions of the geometry and loadings and not of the material type. This conclusion can be used as an important advantage where stress concentration factors can be established using experimental photoelastic tests by making use of a different material other than that used to fabricate a structure.

The stress concentration factors for the flat members mentioned here forth are for 2D stress states i.e. plane stresses and are applicable to very thin sheets where thickness/radius → 0. As this ratio increases, we move towards a plain strain state where the stress at notch increases at the middle of thickness and decreases at the surface.

4 CASE STUDY

4.1 Opposite U-notches in finite width plate

Reliable data is available from strain gage tests (Kikukawa 1962), photoelastic tests (Flynn and Roll 1966), and mathematical analysis (Appl and Koerner 1969) for opposite U notches as can be observed in Chart 1 (Appendix A).

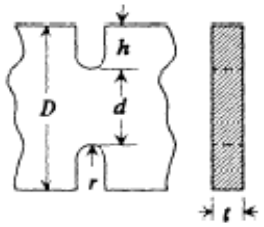

Figure 2: Opposite U notches in finite width thin element

Barrata (1972) matched empirical formulas for K_{tn} with values obtained experimentally and established that these formulas are reasonable for analytical use.

Barrata and Neal (1970)

$$K_t = \left(0.780 + 2.243\sqrt{\frac{h}{r}}\right)\left[0.993 + 0.180\left(\frac{2h}{D}\right) - 1.060\left(\frac{2h}{D}\right)^2 + 1.710\left(\frac{2h}{D}\right)^3\right]\left(1 - \frac{2h}{D}\right)$$

Heywood (1952)

$$K_{tn} = 1 + \left[\frac{h/r}{1.55\,(D/d) - 1.3}\right]^n$$

$$n = \frac{D/d - 1 + 0.5\sqrt{h/r}}{D/d - 1 + \sqrt{h/r}}$$

With h the depth of a notch, h = (D – d) / 2

Referring to Chart 1, the first equation provides values which are in conformity with the solid curves where r/d < 0.25.

In Chart 1 (Appendix A) the range of r/d values from 0 to 0.3, and D/d values from 1 to 2, cover the most extensively used range of parameters which match up with the observations and findings of Kikukawa (1962), Flynn and Roll (1966) and Appl and Koerner (1969). With the

help of significant evidence, it is observed that for larger values of r/d and D/d, the Kt vs D/d plot for corresponding r/d ratio does not level out but attains a peak and then drops gradually to a slightly lower Kt value as D/d approaches infinity. The small effect is not visible in Chart 1.

4.2 Opposite V-notches in finite width plate

As far as geometry is concerned, V shaped notch is of significant importance in mechanical design engineering. It is present in various machine elements. The V shaped notch is also used for stress concentration test pieces for fatigue and fracture tests.

For opposite V-notches in finite width plate, stress concentration factors have been found as a function of the V angle α (Appl and Koerner 1969). According to the Leven-Frocht (1953), $K_{t\alpha}$ and the K_{tu} of a corresponding U notch can be related (Chart 2-Appendix A) which proves that for D/d = 1.66 the angle α has negligible effect up to 90^o.

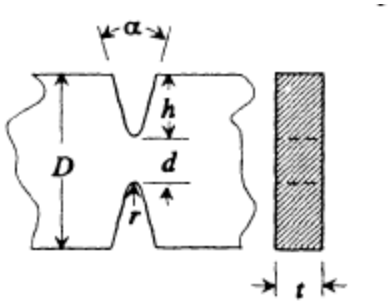

Figure 3: Opposite V notches in finite width thin element

For D=50mm, h= 10mm, r=0.2mm, t=0.05mm, d=30mm, according to the Chart 2.4 and Chart 2.7, we can calculate the stress concentration factor K_t :

$$K_t = C_1 + C_2\frac{2h}{D} + C_3\left(\frac{2h}{D}\right)^2 + C_4\left(\frac{2h}{D}\right)^3 \quad ; \text{Where}$$

$$C_1 = 1.037 + 1.991\sqrt{\frac{h}{r}} + 0.002\,\frac{h}{r}$$

$$C_2 = -1.886 - 2.181\sqrt{\frac{h}{r}} - 0.048\,\frac{h}{r}$$

$$C_3 = 0.649 + 1.086\sqrt{\frac{h}{r}} + 0.142\,\frac{h}{r}$$

$$C_4 = 1.218 - 0.922\sqrt{\frac{h}{r}} - 0.086\,\frac{h}{r}$$

We get C_1= 15.2155, C_2= -19.7080, C_3= 15.4282, C_4= -9.6015 for our case and hence K_t= 9.1863

As per the equation $\sigma_{max} = K_t \sigma_{nom}$ where $\sigma_{nom} = P / td$

- *For Case 1 (Opposite U notches)*, P = 40N,

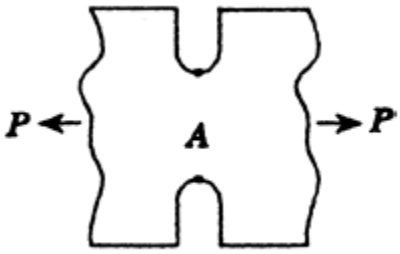

Figure 4 : Case 1 - Axial tension P = 40N applied to opposite U notches in finite width plate

σ_{nom} = 40 / (0.05)(30) = 26.667 MPa

σ_{max} = (9.1863)(26.667) = 244.9683 MPa

- *For Case 2 (Opposite V notches),* P = 40N,

Figure 5: Case 2 - Axial tension P = 40N applied to opposite V notches in finite width plate

σ_{nom} = 40 / (0.05)(30) = 26.667 MPa

σ_{max} = (9.1863)(26.667) = 244.9683 MPa

- *For Case 3 (Opposite V notches)*, P = 100N,

Figure 6: Case 3 - Axial tension P = 100N applied to opposite V notches in finite width plate

σ_{nom} = 100 / (0.05)(30) = 66.667 MPa

σ_{max} = (9.1863)(66.667) = 612.4203 MPa

4.3 Linear FE Analysis of Opposite U notched and V notched plate

4.3.1 Geometric Dimensions

The U notched and V-notched plate is modelled as a symmetric model so the FE analysis is carried out on one of the quadrants in order to save the computation cost and time.

4.3.2 Material Properties

As mentioned before, for plane problems the stress concentration factors are functions of the geometry and loading and not of the type of material. However to proceed with the solution, the material properties entered are as follows:

Young's Modulus, E = 200e9 Pa; Poisson's Ratio, ν = 0.3

4.3.3 Element Type

FEA model of double U and V notched plate was modelled in the global Cartesian coordinate system using PLANE182, PLANE183, SOLID185 and SOLSH190.

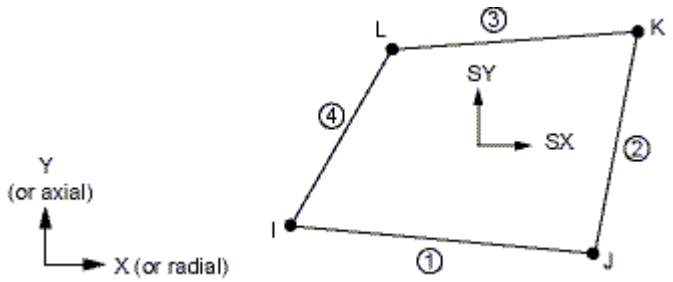

Figure 7: PLANE182 Element [8]

PLANE182 is mostly used for 2-D modeling of solid structures. The element can be used as either a plane element (plane stress, plane strain) or an axisymmetric element. It has four nodes with two degrees of freedom per node i.e. translations in the x and y directions. This element is able to model plasticity, hyperelasticity, stress stiffening, large deflection, and large strain. It also has mixed formulation capability for simulating deformations of nearly incompressible elastoplastic materials, and fully incompressible hyperelastic materials [12].

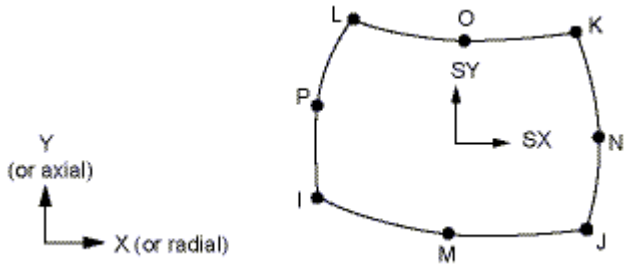

Figure 8: PLANE183 Element [8]

PLANE183 is a higher order 2-D element with eight nodes or six nodes. This element shows quadratic displacement behavior and is more preferred to model meshes that are irregular. For eight or six nodes, each node has two degrees of freedom i.e. translations in the x and y directions. It can also be used as a plane element (plane stress, plane strain and generalized plane strain) or as an axisymmetric element [12].

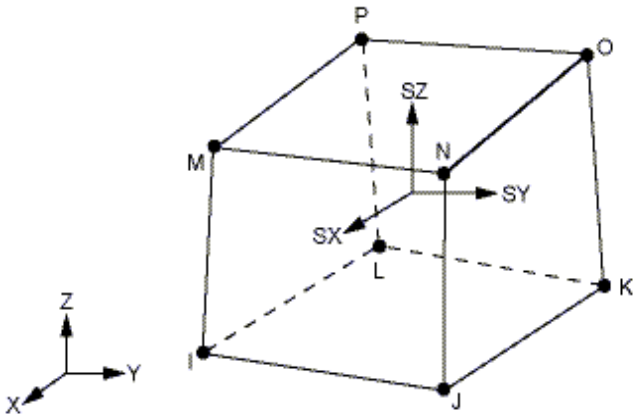

Figure 9: SOLID185 Element [8]

SOLID185 is used for 3-D modeling of solid structures. It consists of eight nodes with three degrees of freedom at each node i.e. translations in the x, y, and z directions. The element offers plasticity, hyperelasticity, stress stiffening, creep, large deflection, and large strain capabilities. It also has mixed formulation capability for simulating deformations of nearly incompressible elastoplastic materials, and fully incompressible hyperelastic materials [12].

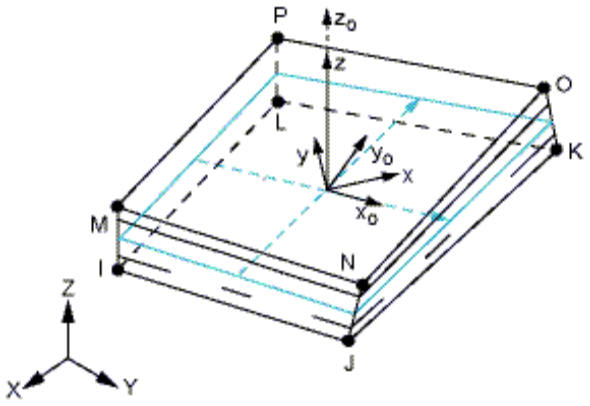

Figure 10: SOLSH190 Element [8]

SOLSH190 is used for shell structures with a variety of thickness ranging from thin to moderately thick elements. This element offers continuum solid element configuration and consists of eight nodes with three degrees of freedom per node i.e. translations in the x, y, and z directions. Therefore no extra effort is required to connect SOLSH190 with other continuum elements. The element provides plasticity, hyperelasticity, stress stiffening, creep, large deflection, and large strain capabilities. For simulating deformations of nearly incompressible elastoplastic materials, and fully incompressible hyperelastic materials, it uses mixed u-P formulation capability. The element evaluation is centered on logarithmic strain and true stress measurements [12].

4.3.4 Shear locking and Hourglassing: Full integration vs Reduced integration

In finite element analysis, shear locking and hourglassing are two main numerical problems because they may result in false solutions for some situations. Fully integrated first order solid elements are overly stiff in bending applications as well as modal analysis and may suffer from shear locking. FEA tool like ANSYS can therefore give us spurious stresses and wrong displacements when fully integrated first order elements are used [20].

It has been shown that the displacement evaluation for linear elastic finite element analysis denotes a lower limit on the strain energy of the system which results in the overestimation of system stiffness matrix. Therefore it might be possible to attain a more accurate result by not calculating the element stiffness matrices exactly in the numerical integration. This likelihood is conceivable if the error in the numerical iteration compensates suitably for the exaggeration of the structural stiffness due to the finite element discretization. Hence, final solutions can be actually improved by reduction in the typical numerical integration order that is used to evaluate

the element stiffness matrices. This theory is stated as reduced integration. This scheme offers a softening effect since higher order polynomial terms will disappear at Guass points of a low order rule, thus excluding these terms from involvement in the system stiffness matrix. Complex displacement modes show less resistance to deformation with less sampling points [21].

However reduced integration is not flawless. Reduced integration first order element leads to a numerical complexity called hourglassing because it can be excessively flexible. Therefore hourglassing has to be appropriately controlled. And if it is not properly controlled, the solutions from this element type cannot be used [20].

For the FE analysis of opposite U and opposite V notches in finite width plate, reduced integration is selected as the element technology. Nevertheless, hourglassing effect is controlled and solution accuracy is checked by refining the mesh and verifying that the ratio of artificial energy to total energy is less than 5%. Plane stress with thickness was designated as the element behavior. Mapped meshing was used.

4.3.5 Boundary Conditions

Symmetric boundary conditions were applied on the left and top side of the geometry. After boundary conditions, pressure having magnitude of -16MPa (Case 1 & Case 2) and -40MPa (Case 3) was applied on the right side.

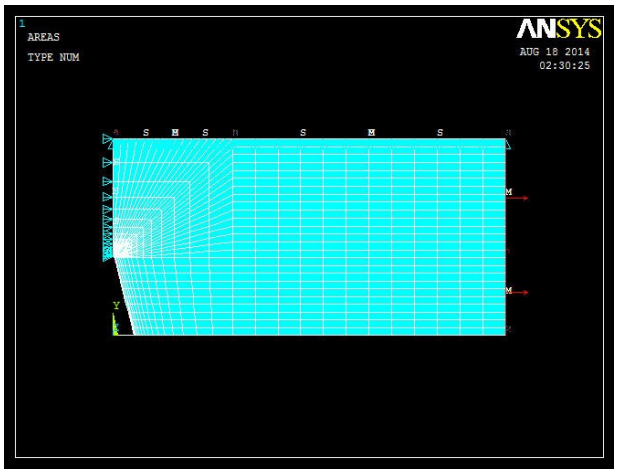

Figure 11: Front view of FE model and boundary conditions

4.3.6 Finite Element Analysis

3D Finite Element Analysis of double U and V notched plate was carried out using SOLID185 and SOLSH190 element type with same boundary conditions and same loading scenarios as applied to the 2D model. The converged maximum stress was found to be overestimated in the same manner as it was observed in the 2D analysis with PLANE182 and PLANE183 element type. However, the computation time increased to a great extent when the number of elements were increased in 3D model to achieve a finer mesh in order to meet the convergence criteria. Therefore the detailed investigation and validation of the proposed methodology was carried out by using PLANE182 element type.

A 2D linear static analysis with PLANE182 element type was performed and mesh was refined several times until the convergence was achieved with the total number of elements reaching up to 230400. This gave the maximum converged value at the top of notch.

4.3.7 Solutions

- *Case 1 (Opposite U notches):P = 40N*

Table 1 shows the convergence of the maximum Von mises stress, maximum stress in X-direction, maximum deflection and total strain energy as the number of elements are increased.

No. of elements	Max. von mises	Max. Sx	Max. deflection	Total Strain Energy
900	158.964	173.664	0.004704	0.0463545
3600	198.324	210.845	0.00470586	0.0463475
14400	234.448	242.570	0.00470616	0.0463456
57600	254.990	259.721	0.00470624	0.0463452
230400	266.818	269.344	0.00470626	0.0463451

Table 1: Case 1 - FE Solution by mesh refinement

Figure 12 shows the trend of the maximum stress as the number of elements increase. Numerical convergence criteria proposed by G.B. Sinclair in [17] and [18] is as follows

1st convergence check:

$$\left|\sigma^{m}_{\max} - \sigma^{c}_{\max}\right| > \left|\sigma^{f}_{\max} - \sigma^{m}_{\max}\right|$$

2nd convergence check:

$$\left|\frac{\sigma^{f}_{\max} - \sigma^{m}_{\max}}{\sigma^{f}_{\max}}\right| < \varepsilon_s$$

ε_s = 0.01 (excellent accuracy), ε_s = 0.05 (good), ε_s = 0.10 (satisfactory)

Where σ^{c}_{max}= Maximum stress for coarse mesh

σ^{m}_{max} = Maximum stress for medium mesh

σ^{f}_{max} = Maximum stress for fine mesh

1st convergence check: (259.721- 242.57) > (269.344- 259.721)

2nd convergence check: (269.344- 259.721) / 269.344 = 0.036 → Good accuracy

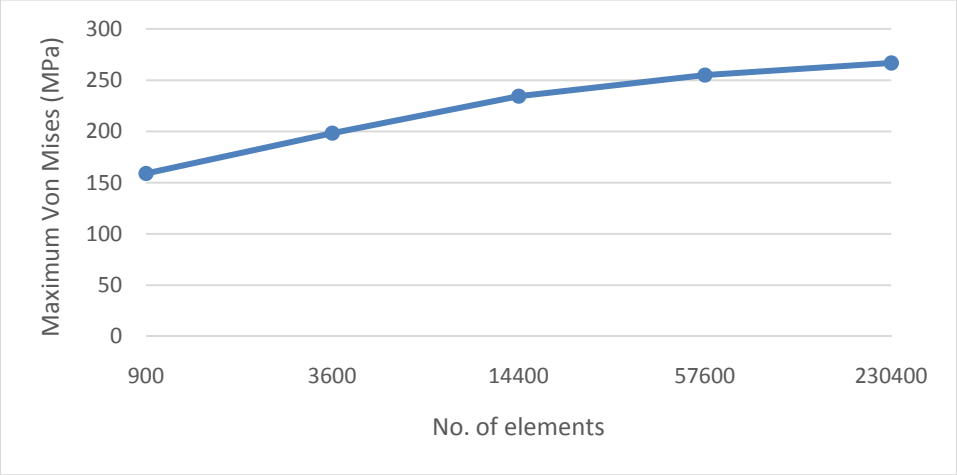

Figure 12: Case 1 - Maximum Von Mises (MPa) vs No. of elements

Figure 13 shows the ANSYS contour plot showing the converged maximum value of stress in x-direction i.e. 269.344 MPa at the tip of the U-notch

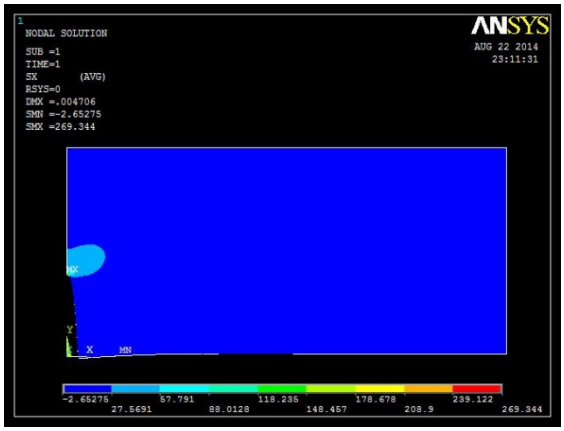

Figure 13: Case 1 - Contour plot - Maximum Stress Sx

- *Case 2(Opposite V notches): P = 40N*

Table 2 shows the convergence of the maximum Von mises stress, maximum stress in X-direction, maximum deflection and total strain energy as the number of elements are increased.

No. of elements	Max. von mises	Max. Sx	Max. deflection	Total Strain Energy
900	156.809	171.457	0.004705	0.0463655
3600	196.258	209.202	0.004707	0.0463580
14400	233.519	241.686	0.004707	0.0463558
57600	254.420	259.171	0.004707	0.0463553
230400	266.383	268.915	0.004707	0.0463552

Table 2: Case 2 - FE Solution by mesh refinement

Figure 14 shows the trend of the maximum stress as the number of elements increase. Numerical convergence criteria proposed by G.B. Sinclair in [17] and [18] is implemented

1st convergence check: (259.171- 241.686) > (268.915- 259.171)

2nd convergence check: (268.915- 259.171) / 268.915 = 0.036 → Good accuracy

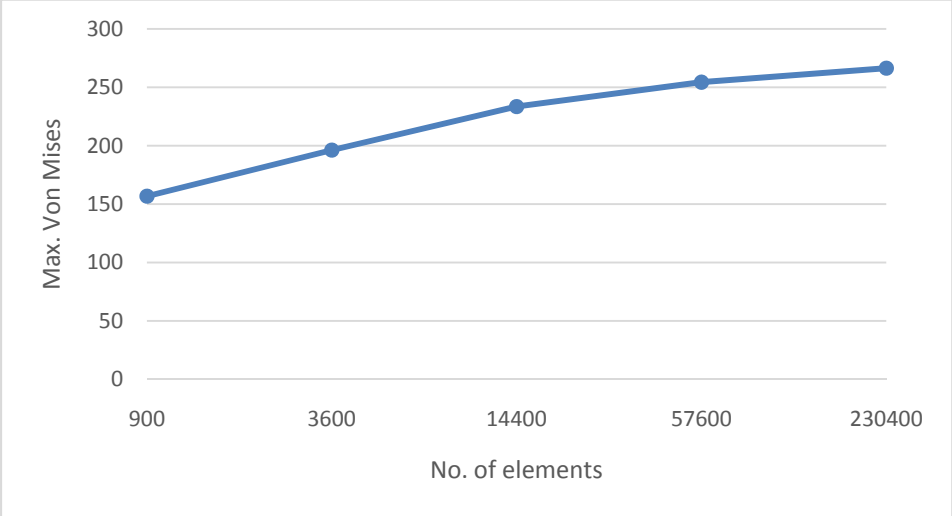

Figure 14: Case 2 - Max. Von Mises (MPa) vs No. of elements

Figure 15 shows the ANSYS contour plot showing the converged maximum value of stress in x-direction i.e. 268.915 MPa at the tip of the V-notch

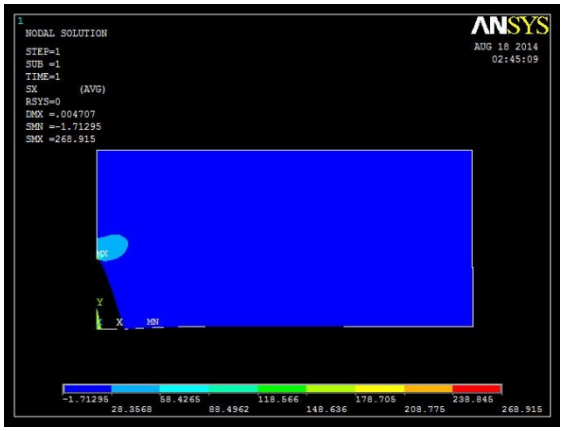

Figure 15: Case 2 - Contour plot - Maximum Stress Sx

- *Case 3 (Opposite V notches):P = 100N*

Table 3 shows the convergence of the maximum Von mises stress, maximum stress in X-direction, maximum deflection and total strain energy as the number of elements are increased.

No. of elements	Max. von mises	Max. Sx	Max. deflection	Total Strain Energy
900	392.023	428.643	0.011762	0.289784
3600	491.645	523.005	0.011767	0.289737
8100	548.681	573.921	0.011768	0.289727
14400	583.797	604.214	0.011768	0.289724
57600	636.049	647.928	0.011768	0.289721
230400	665.958	672.286	0.011768	0.289720

Table 3: Case 3 - FE solution by mesh refinement

Figure 16 shows the trend of the maximum stress as the number of elements increase. Numerical convergence criteria proposed by G.B. Sinclair in [17] and [18] is implemented

1st convergence check: (647.928 - 604.214) > (672.286 - 647.928)

2nd convergence check: (672.286 - 647.928) / 672.286 = 0.036 → Good accuracy

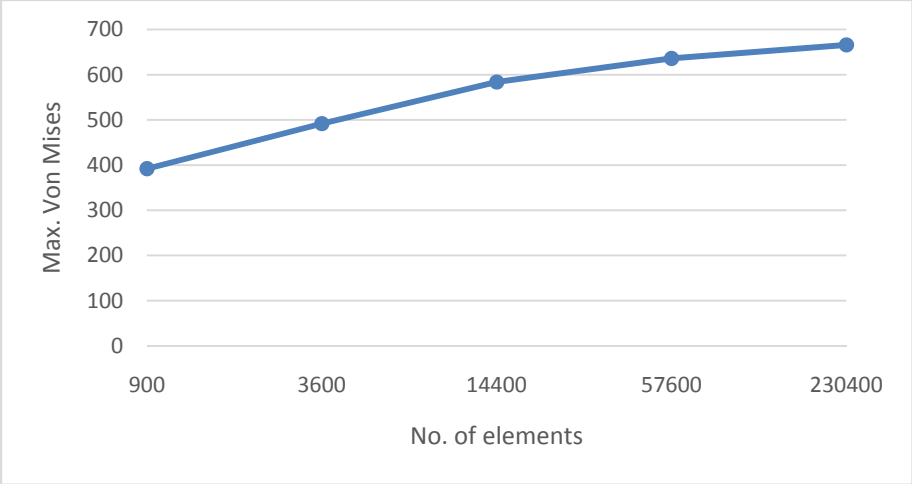

Figure 16: Case 3 - Max. Von Mises (MPa) vs No. of elements

Figure 17 shows the ANSYS contour plot showing the converged maximum value of stress in x-direction i.e. 268.915 MPa at the tip of the V-notch

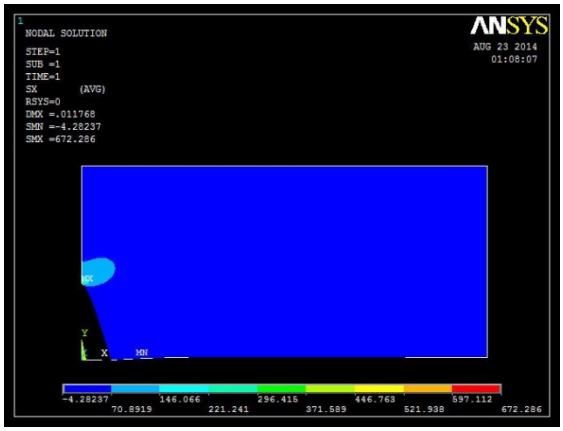

Figure 17: Case 3 - Contour plot - Maximum Stress Sx

Evaluating the empirical solutions derived from the experimental photoelastic tests using the geometric dimensions, the maximum stress according to the formula is calculated as 244.968 MPa for Case 1 and Case 2; 612.420 MPa for Case 3. From ANSYS, we have obtained the converged maximum stress the value of as 269.344 MPa for Case 1, 268.915 MPa for Case 2 and 672.286 MPa for Case 3.

4.3.8 FEA Stress concentration factor [19]

The area under the two stress gradient curves i.e. the stress concentration and uniform stress field must be equal according to the principle of equivalent energy. It is known that the area under the uniform stress field curve $A_{Kt} = \sigma_{nom} * Distance$.

For FEA, we can get this A_{Kt} in ANSYS by using path operations and selecting the nodes to define the path which is the distance from the notch tip to the center of the plate. This is followed by the application of integration calculations on mapped path item i.e. Sx (stress in x direction) in our case to find the area (Appendix B). Solving for σ_{nom}, $\sigma_{nom} = A_{Kt} / Distance$

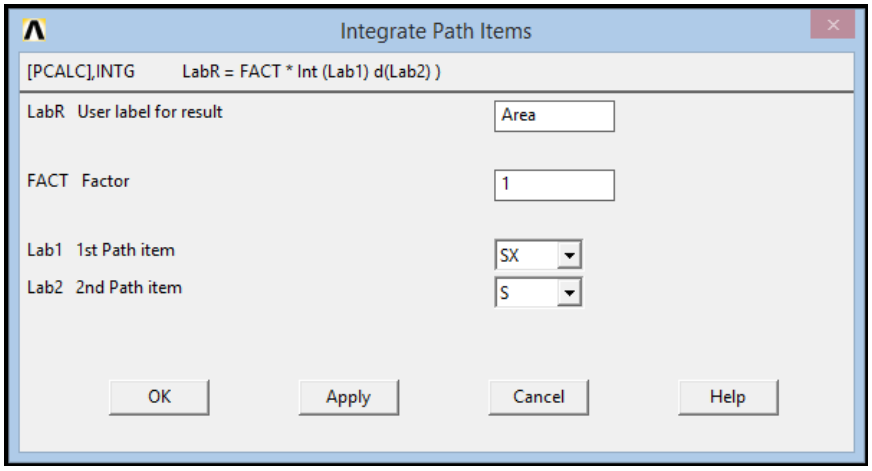

Figure 18: Using integration on mapped path items

Case 1(Opposite U notches): P=40N

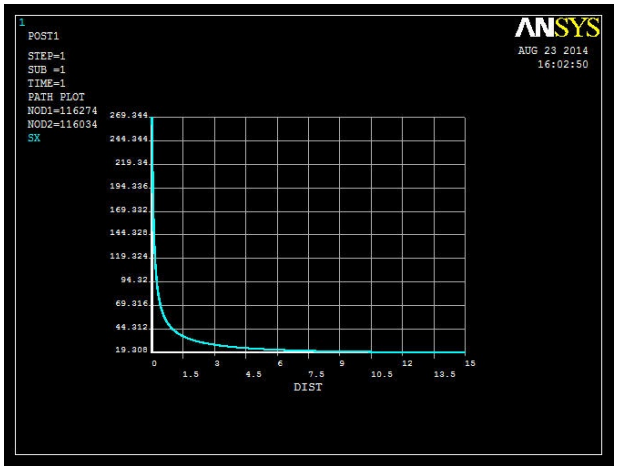

Figure 19: Case 1-Stress (Sx) vs Distance plot in ANSYS

As we know AKt= σnom* Distance, σnom = AKt / Distance = 400.01 / 15 = 26.6673 MPa

So the FEA Kt for double V notched plate will be σmax/σnom = 269.34 / 26.6673 = 10.10

% Error (Formula – FEA) = (9.1863-10.10)/9.1863 *100 = -9.946%

Case 2 (Opposite V notches):P=40N

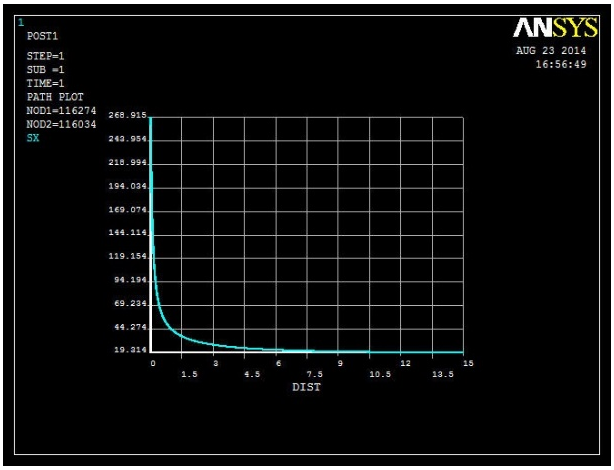

Figure 20: Case 2-Stress (Sx) vs Distance plot in ANSYS

As we know AKt= σnom* Distance, σnom = AKt / Distance = 400.01 / 15 = 26.6673 MPa

So the FEA Kt for double V notched plate will be σmax/σnom = 268.91 / 26.6673 = 10.0839

% Error (Formula – FEA) = (9.1863-10.0839)/9.1863 *100 = -9.8070%

Case 3 (Opposite V notches): P=100N

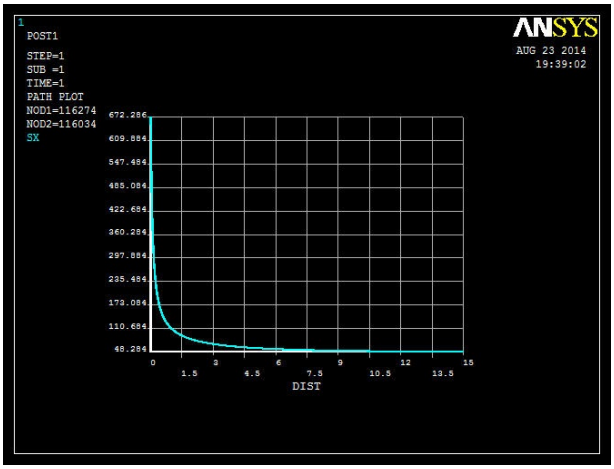

Figure 21: Case 3 - Stress (Sx) vs Distance plot in ANSYS

As we know AKt= σnom* Distance, σnom = AKt / Distance = 1000 / 15 = 66.667 MPa

So the FEA Kt for double V notched plate will be σmax/σnom = 672.286 / 66.667 = 10.0842

% Error (Formula – FEA) = (9.1863-10.0842)/9.1863 *100 = -9.7748%

4.3.9 Linear FEA with different notch radii

For Case 1, linear finite element analysis was carried out for geometries with different notch radii to evaluate the trend of maximum stress overestimation as the radius of the notch was increased.

Radius(mm)	h/r	Force(N)	Kt (Formula)	Max. Stress (Formula)	Kt (FEA)	Max. Stress (FEA)
0.2	50	40	9.1863	244.968	10.101	269.344
0.4	25	55	6.6316	243.160	7.334	268.912
1	10	84	4.3648	244.429	4.845	271.313

Table 4: Maximum stress analysis with variation of notch radius

As it can be observed from Table 4, the maximum stress in the assembly of opposite U notches in finite width plate obtained by linear finite element analysis is found to be overestimated in the same manner as radius is increased when compared to the maximum stress value evaluated by the empirical solutions based on the experimental photoelastic tests.

5 Stress Resolving Methodology

5.1 Bilinear Analysis

The proposed stress resolving technique to eliminate overestimated stress concentration consists of the following steps.

- A linear finite element analysis is conducted while specifying only the material properties for a linear material model without specifying yield stress of the material.
- After ensuring that convergence has been achieved, the overestimated maximum stress value is recorded.
- A nonlinear material model is then introduced and yield stress of the material is specified less than the maximum stress which is decreased successively in the subsequent iterations while the results are analyzed. With the yield stress having a decreasing trend, the maximum stress levels also get reduced. At the same time there is an increase in the overall deflection and total strain energy. Thus, this yield drop has to be limited up to a value where distribution of stress remains uniform and the change in deformation and total strain energy is linear. The maximum stress at point where the drop in yield stress is limited will be the resolved stress.

6 Results

6.1 Computational Results

Case 1 (Opposite U notches): P=40N

As seen in the table the overestimated stress concentration was resolved by artificially introducing a nonlinear material model and dropping the material's yield strength below the maximum stress produced. In successive iterations, it can be observed that by reducing the yield stress of the material, the stress levels decline and at the same time the overall deflection and total strain energy increases.

Case	Yield Strength (MPa)	Max. (Von Mises)	Max.Sx	% Error Kt	Deflection (mm)	% change in deflection	Total Strain Energy	% change in total strain energy
Linear		266.818	269.344	-9.949	0.00470626	0	0.0463451	0
	270	266.818	269.344	-9.949	0.00470626	0	0.0463451	0
	265	265	267.565	-9.223	0.00470627	0.0002125	0.0463451	0
	260	260	262.523	-7.165	0.00470627	0.0002125	0.0463452	0.000216
	255	255	257.485	-5.108	0.00470628	0.000425	0.0463454	0.000647
	250	250	253.551	-3.502	0.00470629	0.0006374	0.0463455	0.000863
Resolved	245	245	249.672	-1.919	0.00470630	0.0008499	0.0463457	0.001295
	240	240	244.496	0.194	0.00470632	0.0012749	0.0463462	0.002373
	235	235	241.812	1.290	0.00470635	0.0019123	0.0463466	0.003237
	230	230	238.223	2.755	0.00470637	0.0023373	0.0463471	0.004315
	225	225	233.250	4.785	0.00470640	0.0029748	0.0463476	0.005394
	220	220	230.769	5.797	0.00470645	0.0040372	0.0463485	0.007336

Table 5: Case 1 - Stress resolving by dropping yield of material

Overestimated maximum stress value of 269.344 MPa was observed in linear FEA and that value has been reduced to around 244.496 MPa which is the resolved stress in this case. Drop in yield stress of material is limited where the change in overall deformation and total strain energy starts showing non-linear behavior and starts increasing drastically.

Percent change in deformation was calculated according to

$$\% \text{ change in deformation} = \frac{(\text{Resolved Case Deformation} - \text{Base Case Deformation})}{\text{Base Case Deformation}} \times 100$$

Percentage change in total strain energy was calculated according to

$$\% \text{ change in total strain energy} = \frac{(\text{Resolved Case TSE} - \text{Base Case TSE})}{\text{Base Case TSE}} \times 100$$

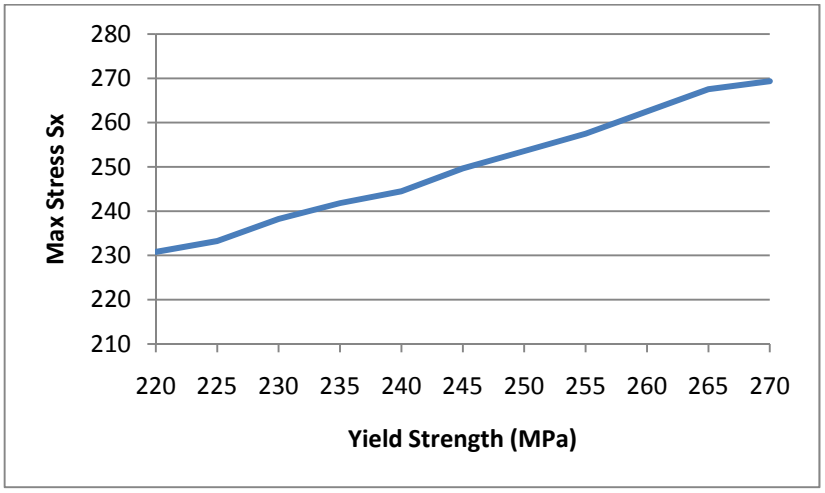

Figure 22: Case 1 - Max. Stress (Sx) vs Yield Strength (MPa)

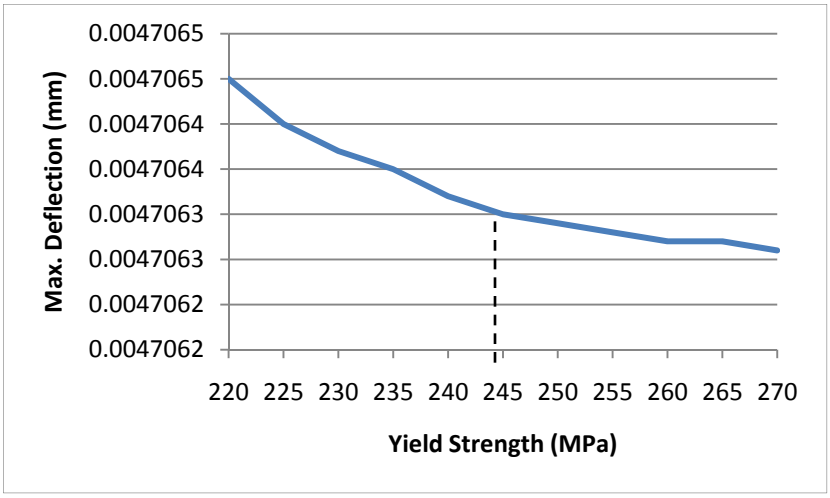

Figure 23: Case 1 - Maximum Deformation vs Yield Strength

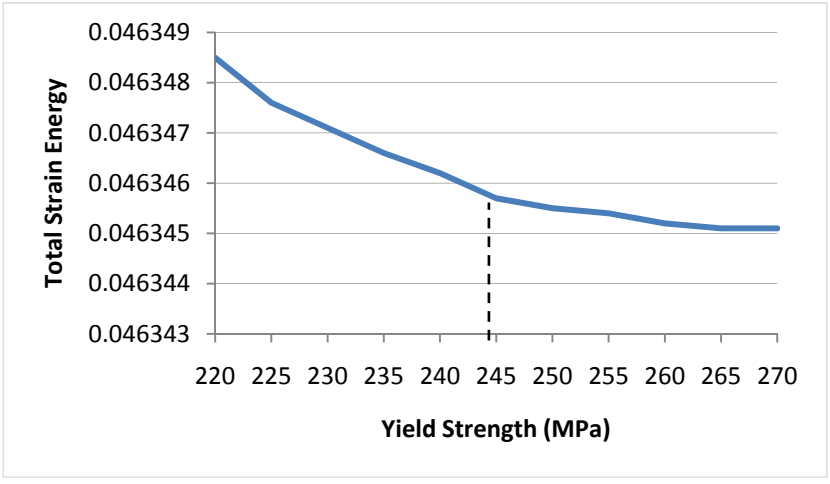

Figure 24: Case 1 - Total Strain Energy vs Yield Strength

Case 2 (Opposite V notches): P=40N

As seen in the table the overestimated stress concentration was resolved by artificially introducing a nonlinear material model and dropping the material's yield strength below the maximum stress produced. In successive iterations, it can be observed that by reducing the yield stress of the material, the stress levels decline and at the same time the overall deflection and total strain energy increases.

Case	Yield Strength (MPa)	Max. Stress (Von Mises)	Max. Sx	% Error Kt	Deflection (mm)	% change in deflection	Total Strain Energy	% change in total strain energy
Linear		266.383	268.915	-9.77419	0.00470726	0	0.0463552	0
	270	266.383	268.915	-9.77419	0.00470726	0	0.0463552	0
	265	265	267.576	-9.2276	0.00470726	0	0.0463552	0
	260	260	262.535	-7.1698	0.00470726	0	0.0463553	0.0002157
	255	255	257.495	-5.11242	0.00470727	0.000212	0.0463554	0.0004314
	250	250	253.335	-3.41426	0.00470728	0.000425	0.0463556	0.0008629
Resolved	245	245	249.661	-1.91449	0.00470729	0.000637	0.0463558	0.0013
	240	240	244.505	0.190252	0.00470731	0.001062	0.0463562	0.0022
	235	235	241.594	1.378556	0.00470734	0.0017	0.0463567	0.0032
	230	230	238.215	2.757902	0.00470736	0.002124	0.0463571	0.0041
	225	225	233.241	4.788346	0.00470739	0.002762	0.0463576	0.0052
	220	220	230.569	5.879087	0.00470744	0.003824	0.0463585	0.0071

Table 6: Case 2 - Stress resolving by dropping yield of material

Overestimated maximum stress value of 268.915 MPa was observed in linear FEA and that value has been reduced to around 244.505 MPa which is the resolved stress in this case. Drop in yield stress of material is limited where the change in overall deformation and total strain energy starts showing non-linear behavior and starts increasing drastically.

Percent change in deformation was calculated according to

$$\% \text{ change in deformation} = \frac{(\text{Resolved Case Deformation} - \text{Base Case Deformation})}{\text{Base Case Deformation}} \times 100$$

Percentage change in total strain energy was calculated according to

$$\% \text{ change in total strain energy} = \frac{(\text{Resolved Case TSE} - \text{Base Case TSE})}{\text{Base Case TSE}} \times 100$$

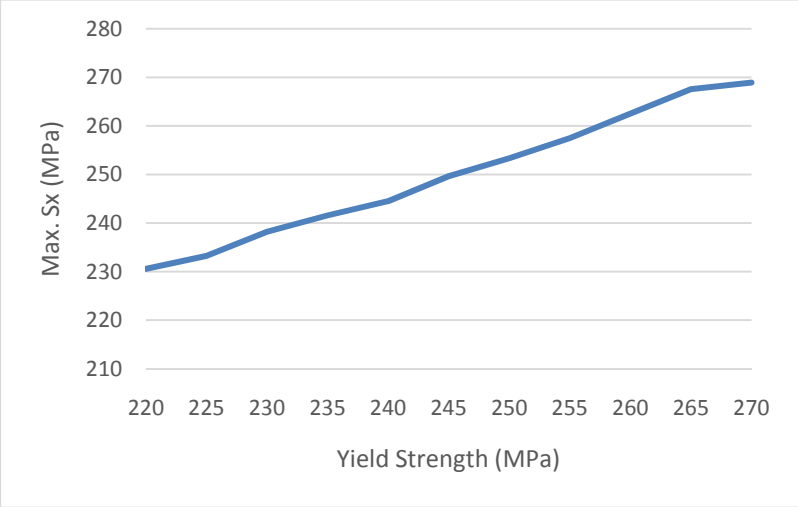

Figure 25: Case 2 - Maximum Stress (Sx) vs Yield Strength

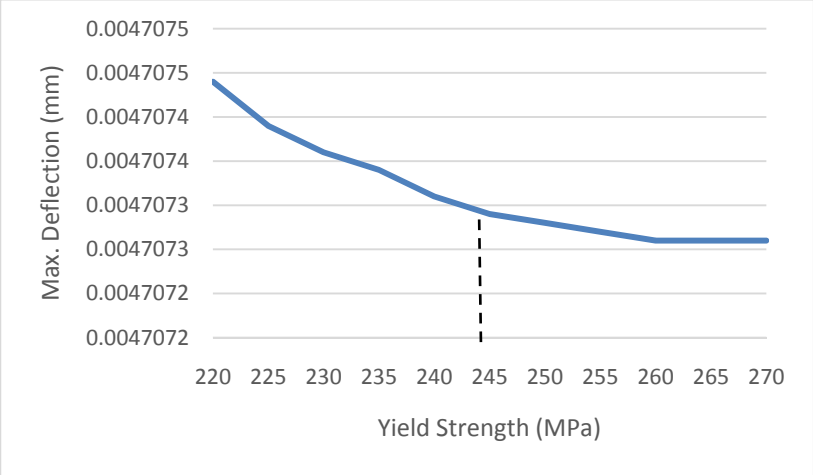

Figure 26: Case 2 - Maximum Deformation vs Yield Strength

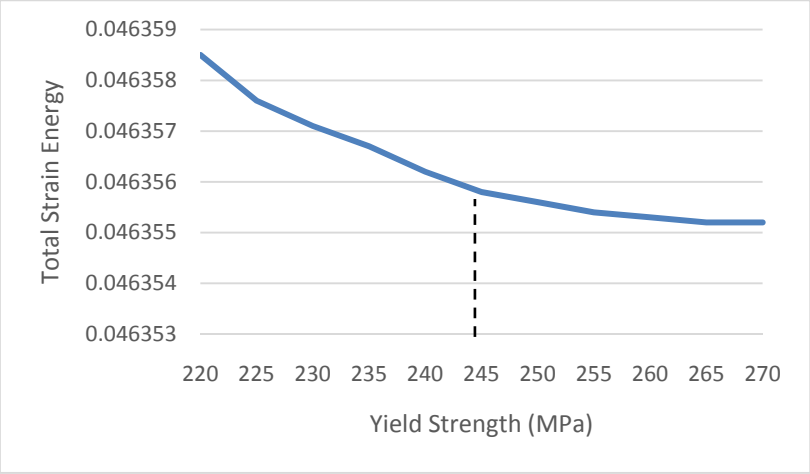

Figure 27: Case 2 -Total Strain Energy vs Yield Strength

Case 3(Opposite V notches): P=100N

As seen in the table the overestimated stress concentration was resolved by artificially introducing a nonlinear material model and dropping the material's yield strength below the maximum stress produced. In successive iterations, it can be observed that by reducing the yield stress of the material, the stress levels decline and at the same time the overall deflection and total strain energy increases.

Case	Yield Strength (MPa)	Max Von Mises	Max. Sx	% Error Kt	Deflection (mm)	% change in deflection	Total Strain Energy	% change in total strain energy
Linear		665.958	672.286	-9.7748	0.01176814	0	0.289720	0
	680	665.958	672.286	-9.7748	0.01176814	0	0.289720	0
	670	665.958	672.286	-9.7748	0.01176814	0	0.289720	0
	660	660	666.42	-8.8169	0.01176815	8.49752E-05	0.289720	0
	650	650	656.336	-7.1704	0.01176816	0.00016995	0.289721	0.000345
	640	640	646.257	-5.5246	0.01176817	0.000254926	0.289721	0.000345
	630	630	636.181	-3.8793	0.01176819	0.000424876	0.289722	0.00069
	620	620	631.064	-3.0438	0.01176821	0.000594826	0.289723	0.001035
Resolved	610	610	621.725	-1.5189	0.01176823	0.000764777	0.289724	0.001381
	600	600	611.263	0.18942	0.01176828	0.001189653	0.289726	0.002071
	590	590	605.013	1.20996	0.01176833	0.001614529	0.289729	0.003106
	580	580	600.5	1.94687	0.01176838	0.002039405	0.289731	0.003797
	570	570	590.567	3.56878	0.01176843	0.002464281	0.289733	0.004487
	560	560	585.151	4.45314	0.01176851	0.003144082	0.289737	0.005868
	550	550	576.423	5.8783	0.01176860	0.003908859	0.289741	0.007248
	540	540	567.24	7.37775	0.01176871	0.004843586	0.289746	0.008974

Table 7: Case 3 - Stress resolving by dropping yield of material

Overestimated maximum stress value of 672.286 was observed in linear FEA and that value has been reduced to around 621.725 MPa which is the resolved stress in this case. Drop in yield stress of material is limited where the change in overall deformation and total strain energy starts showing non-linear behavior and starts increasing drastically. .

Percent change in deformation was calculated according to

$$\% \text{ change in deformation} = \frac{(\text{Resolved Case Deformation} - \text{Base Case Deformation})}{\text{Base Case Deformation}} \times 100$$

Percentage change in total strain energy was calculated according to

$$\% \text{ change in total strain energy} = \frac{(\text{Resolved Case TSE} - \text{Base Case TSE})}{\text{Base Case TSE}} \times 100$$

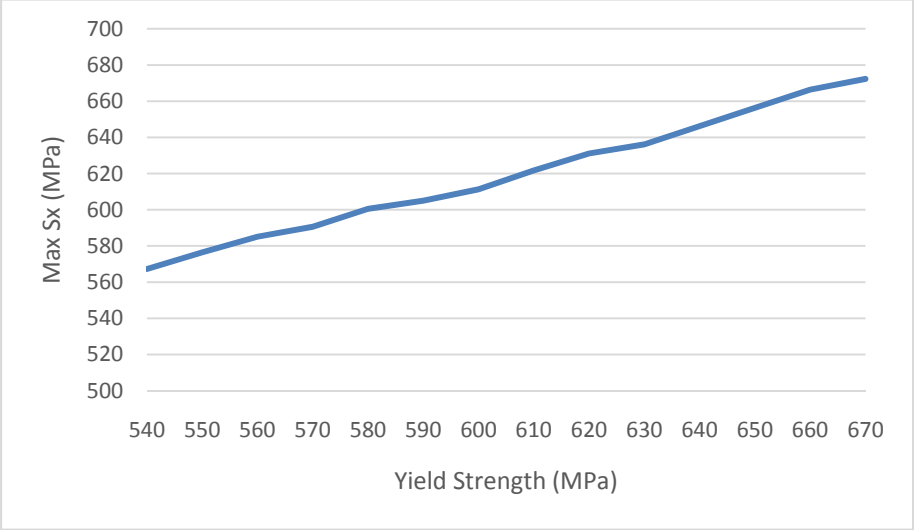

Figure 28: Case 3 - Maximum Stress (Sx) vs Yield Strength

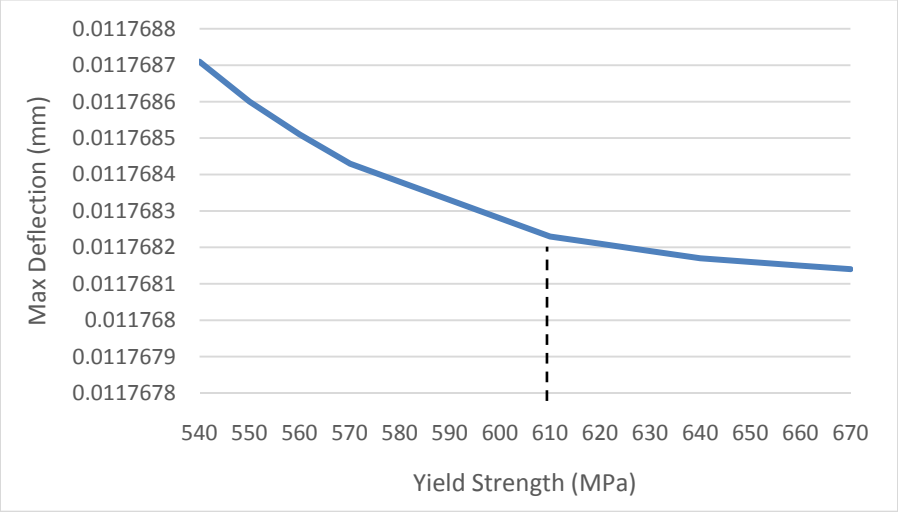

Figure 29: Case 3 - Maximum Deformation vs Yield Strength

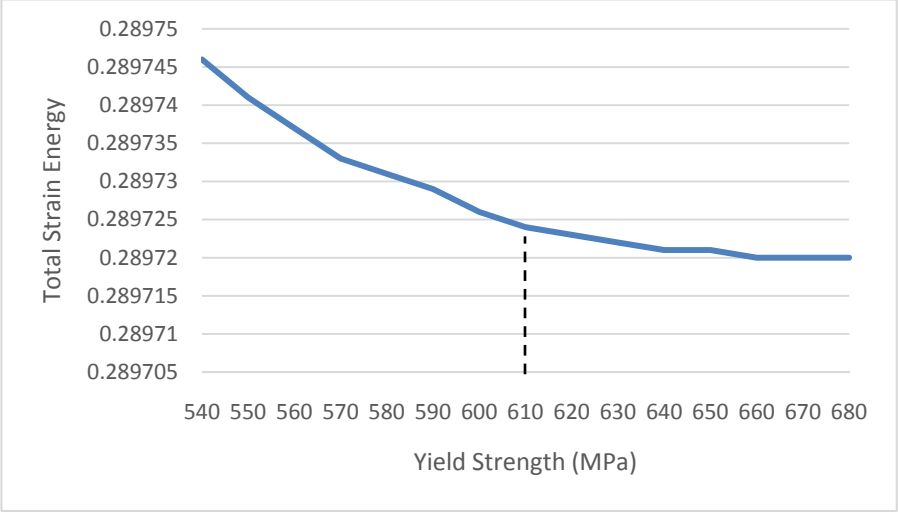

Figure 30: Case 3 - Total Strain Energy vs Yield Strength

7 Conclusions and Advantages

In this scheme, the fundamental idea was based on initiation of material flow in a localized region in the vicinity of maximum stress by using a nonlinear material model. Specifying the yield stress of the material less than the maximum stress in subsequent iterations reduced the unreal and overestimated stress concentration at the notch tip. By decreasing yield stress of the material in FE model artificially, overall deformation and total strain energy increases as expected. However, the vital feature of this methodology that needs to be highlighted is the limiting value to which change in overall deformation and total strain energy can be permitted for the stress to be termed as resolved. As it can be observed, this increase in overall deformation and total strain energy happens slowly and gradually up to a limit and that is the limit of the yield drop. It is recommended that the yield drop is limited to the point where the change in overall deformation and total strain energy starts behaving nonlinearly and begins to increase exponentially. The resolved stress by this technique is found to be near the maximum stress value that was calculated by the formula.

Hence it can be concluded that by inducing an artificial nonlinear material model according to this methodology, overestimated FEA stress concentrations were resolved with negligible change in the deformation and total strain energy. In this study, validation was carried out with the available experimental solutions. This technique is not dependent on the type of material and loading. It should be clearly understood that yielding is not taking place in the real problem. As it was mentioned before the main goal of mechanical design is to keep the stresses within linear elastic region and to ensure that the maximum stresses are less than the yield limit.

The method presented in this study to eliminate unreal and overestimated stress concentration in an FE model was validated on a simple and conventional model but it can also be applied for resolving overestimated stress concentration observed in similar class of complex structures. FEA is being widely used for evaluation and validation of mechanical designs and the proposed technique offers an application oriented working solution for an improved mechanical design by appropriately analyzing true stress distribution in the structure.

This stress resolving technique is advantageous in many ways. Overestimated stress concentration was economically resolved without changing the geometry of the FE model. As a result the structural design was improved and this lead to the prediction of true material response. Consequently several critical geometric parameters like thickness can be adjusted accordingly. At the same time the material can be selected in view of the resolved maximum stress. This can prove to be quite beneficial since reduced cost of material and weight of the structure are critical for aerospace applications. Finally, this methodology provides a greater margin for improvement in the safety factor as the maximum design load is resolved.

Bibliography

[1]. Topac M., Enginar H., Kuralay N., Reduction of stress concentration at the corner bends of the antiroll bar by using parametric optimization, Mathematical and computational applications, Vol. 1, 2011

[2]. David Taylor, Andrew Kelly, Matteo Toso, Luca Susmel, The Variable Radius Notch: Two New Methods for Reducing Stress Concentration, Engineering Failure Analysis, December 2010 10.1016/j.engfailanal.2010.12.012

[3]. Monika G. Garrell, Albert J. Shih, Edgar Lara Curzio, Ronald O. Scattergood, Finite-Element analysis of stress concentration in ASTM D638 tension specimens, Journal of testing and evaluation, Vol. 31.

[4] Warren C. Young, Richard G. Budynas, Roark's Formulas for Stress and Strain, 7th Edition

[5]. Tirupathi R. Chandrupatla, Ashok D. Belegundu, Introduction to Finite Elements in Engineering, Prentice Hall, 2002

[6]. David V. Hutton, Fundamentals of Finite Element Analysis, 1st Edition, McGraw Hill 2004

[7]. G.B. Sinclair, J.R. Beisheim, S. Sezer, Practical Convergence-Divergence Checks for Stresses from FEA, International ANSYS Conference 2006.

[8]. ANSYS Release 13.0 Documentation. Contact Technology Guide: ANSYS Inc., 2010

[9]. Zhichao Wang, Don Draper, Jianxiong Chen, How to Achieve Quick and Accurate FE Solution Small Radius Removal and Element Size, Intl. ANSYS Conference 2006

[10]. Paul Kurowski, Design Generator Inc., Ontario, Canada, Easily made errors mar FEA results, http://machinedesign.com/archive/easily-made-errors-mar-fea-results

[11]. Paul Kurowski, Genexis Design Inc., Ontario, Canada, More errors that mar FEA results, http://machinedesign.com/archive/more-errors-mar-fea-results

[12]. ANSYS Release 13.0 Theory Reference, ANSYS Inc. 2010

[13]. ANSYS – Fundamental FEA Concepts and Applications. A Guidebook for the Use and Applicability of Workbench Simulation Tools from ANSYS, Inc.

[14]. J. R. Beisheim, G. B. Sinclair, Three-Dimensional Submodeling of Stress Concentrations

[15]. Joseph J. Rencis, Sachin Terdalkar, University of Arkansas, Stress Concentrations and Static Failure for Common Elements used in Finite Element Stress Analysis

[16]. Peterson's Stress Concentration Factors, 3rd Edition, Walter D. Pilkey, Deborah F. Pilkey

[17]. G.B. Sinclair, D. Mullan, A simple yet accurate finite element procedure for computing stress intensity factors. International Journal for Numerical Methods in Engineering, 1982, Vol. 18, pp.1587-1600.
[18]. N.G. Cormier, B.S. Smallwood, G.B. Sinclair, G. Meda, Aggressive Submodelling of stress Concentrations. International Journal for Numerical Methods in Engineering, 1999, Vol. 46, pp. 889-909
[19]. W.D.Growney, Using FEA results to determine stress concentration factors, 2008 International ANSYS Conference
[20]. Eric Quili Sun, Shearlocking and hourglassing in MSC Nastran, ABAQUS and ANSYS
[21].http://personal.egr.uri.edu/sadd/mce561/2D%20Elasticity%20Computational%20Issues.pdf

Appendix A- Charts

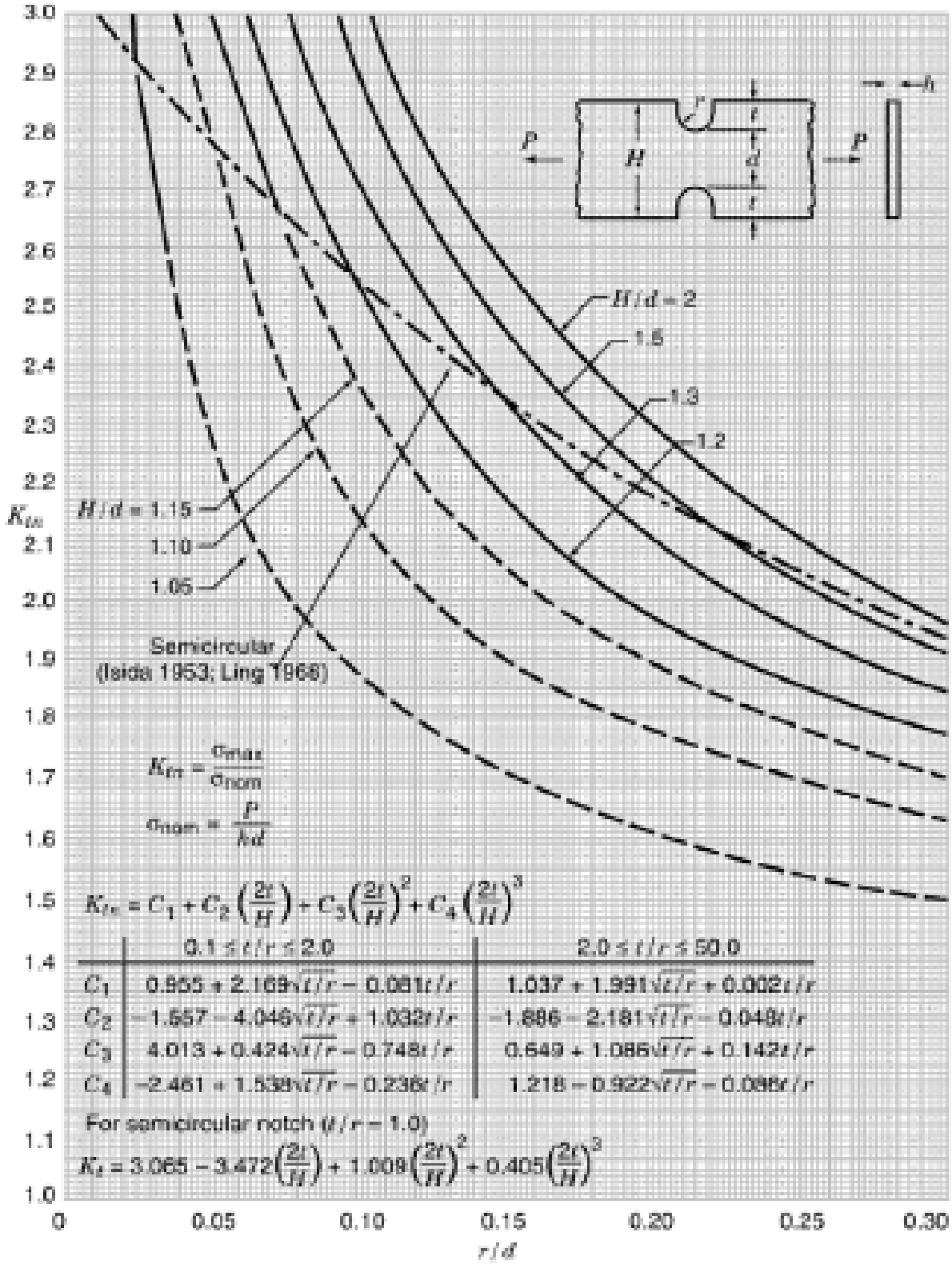

Chart 1: Stress concentration factor for flat tension bar with opposite U shaped notches [16]

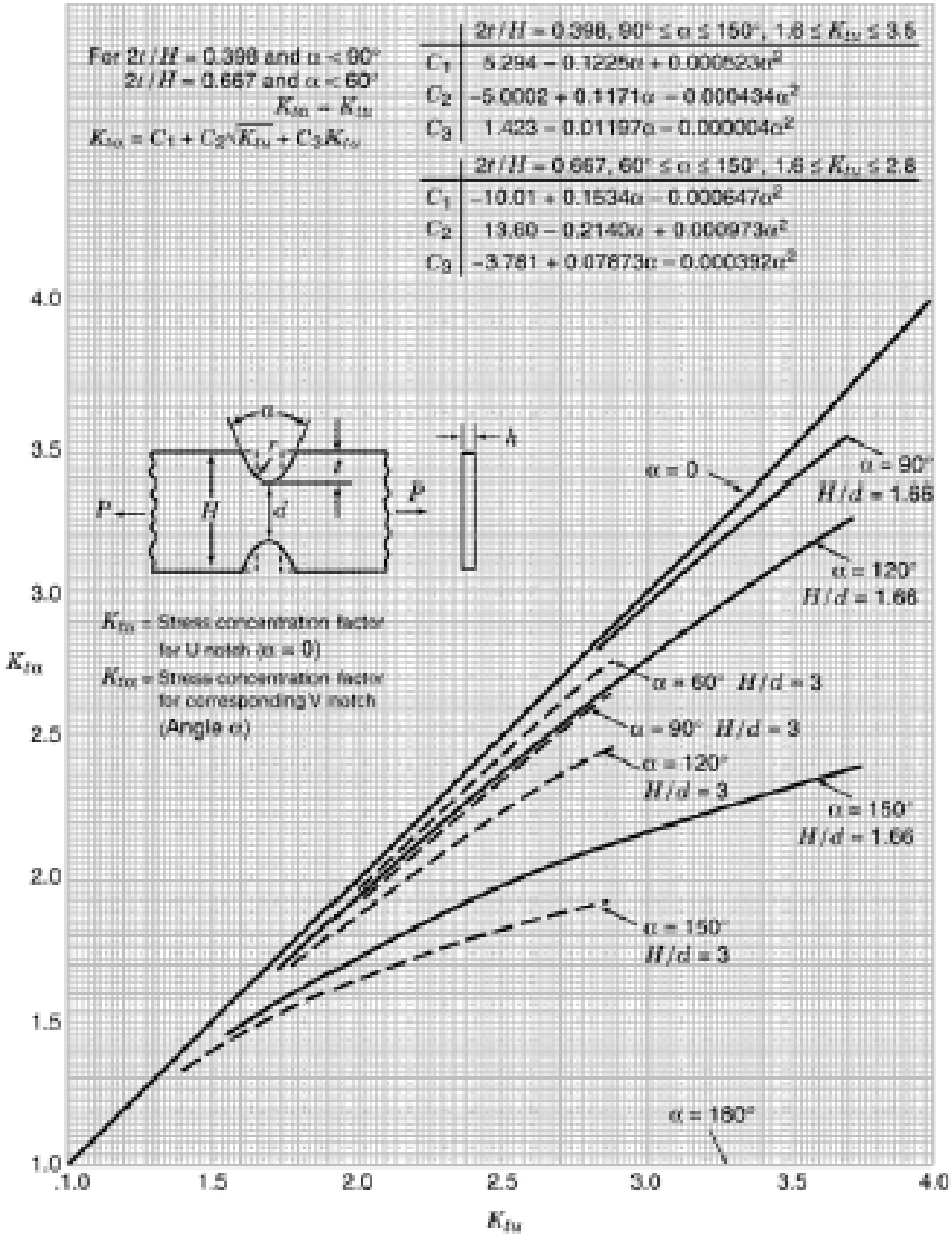

Chart 2: Stress concentration factor for flat tension bar with opposite V shaped notches [16]

Appendix B - Tables

S	SX	AKt
0	269.34	0
2.00E-02	235.14	5.0743
4.02E-02	202.16	9.4777
6.02E-02	177.98	13.281
8.01E-02	159.51	16.618
0.10005	144.76	19.652
0.50009	62.181	54.927
1.0006	43.829	80.591
1.5004	36.344	100.42
2.0005	32.109	117.45
2.5007	29.344	132.78
3.001	27.385	146.95
3.5007	25.924	160.25
4.0004	24.791	172.91
4.5019	23.887	185.1
5.0004	23.156	196.82
5.5016	22.55	208.27
6.0026	22.044	219.44
6.5008	21.618	230.31
7.0003	21.256	241.02
7.5015	20.944	251.59
8.0005	20.677	261.97
8.5051	20.444	272.35
9.0065	20.244	282.55
9.5009	20.073	292.51
10.006	19.922	302.61
10.506	19.794	312.54
11.006	19.684	322.4
11.503	19.591	332.17
12.004	19.513	341.97
12.508	19.448	351.78
13.004	19.397	361.41
13.5	19.358	371.02
14.003	19.33	380.76
14.504	19.314	390.43
15	19.308	400.01

Table 8: List of path items for Case 1

S	SX	AKt
0	268.91	0
1.03E-02	254.54	2.705
2.00E-02	234.76	5.0661
4.02E-02	201.83	9.4624
6.02E-02	177.69	13.259
8.01E-02	159.26	16.591
0.10005	144.54	19.621
0.50009	62.199	54.875
1.0006	43.845	80.549
1.5004	36.35	100.38
2.0005	32.11	117.42
2.5007	29.343	132.74
3.001	27.383	146.91
3.5007	25.922	160.21
4.0004	24.79	172.87
4.5019	23.886	185.07
5.0004	23.157	196.79
5.5016	22.551	208.24
6.0026	22.045	219.4
6.5008	21.62	230.28
7.0003	21.258	240.98
7.5015	20.947	251.56
8.0005	20.68	261.94
8.5051	20.447	272.32
9.0065	20.248	282.52
9.5009	20.077	292.49
9.5078	20.075	292.62
10.006	19.927	302.59
10.506	19.799	312.52
11.006	19.689	322.38
11.503	19.596	332.15
12.004	19.518	341.95
12.508	19.453	351.77
13.004	19.402	361.4
13.5	19.363	371.01
14.003	19.335	380.75
14.504	19.319	390.43
15	19.314	400.01

Table 9: List of path items for Case 2

S	SX	AKt
0	672.29	0
2.00E-02	586.89	12.665
4.02E-02	504.58	23.656
6.02E-02	444.23	33.148
6.07E-02	443.12	33.341
8.01E-02	398.15	41.478
0.10005	361.36	49.051
0.50009	155.5	137.19
1.0006	109.61	201.37
1.5004	90.875	250.96
2.0005	80.275	293.55
2.5007	73.358	331.86
3.001	68.458	367.27
3.5007	64.805	400.53
4.0004	61.975	432.18
4.5019	59.716	462.67
5.0004	57.891	491.96
5.5016	56.377	520.59
6.0026	55.113	548.51
6.5008	54.051	575.7
7.0003	53.145	602.46
7.5015	52.367	628.9
8.0005	51.7	654.85
8.5051	51.118	680.79
9.0065	50.619	706.3
9.5009	50.193	731.21
10.006	49.816	756.46
10.506	49.496	781.3
11.006	49.222	805.96
11.503	48.99	830.37
12.004	48.794	854.88
12.508	48.632	879.43
13.004	48.505	903.51
13.5	48.408	927.53
14.003	48.338	951.88
14.504	48.298	976.07
15	48.284	1000

Table 10: List of path items for Case 3

Appendix C- Contour plots for Linear FEA

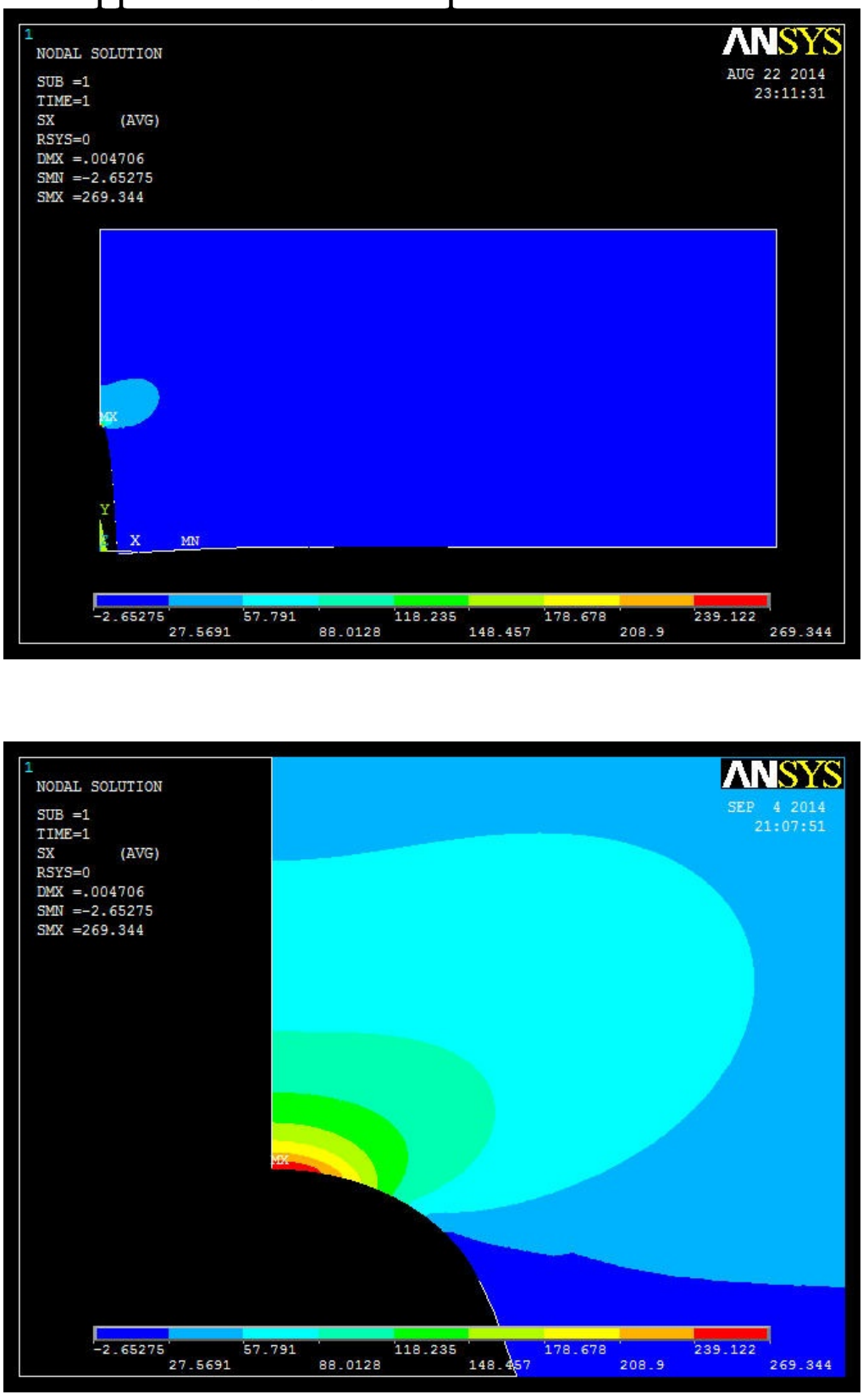

Figure 31: Stress (Sx) plot for Case 1

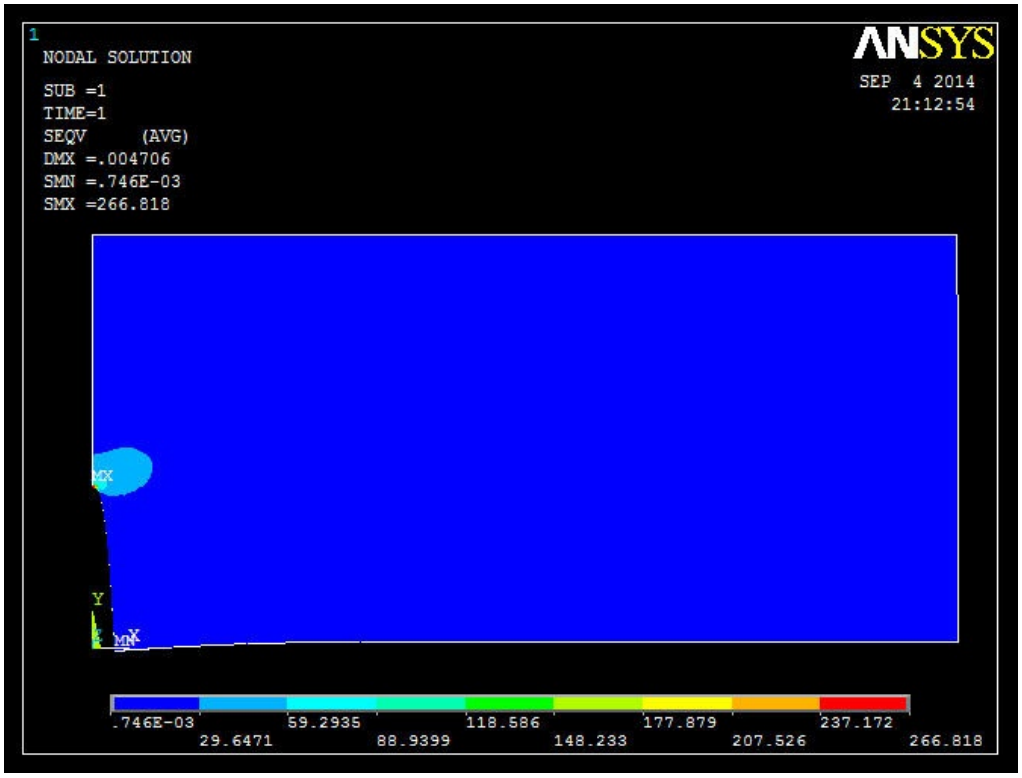

Figure 32: Von Mises Stress plot for Case 1

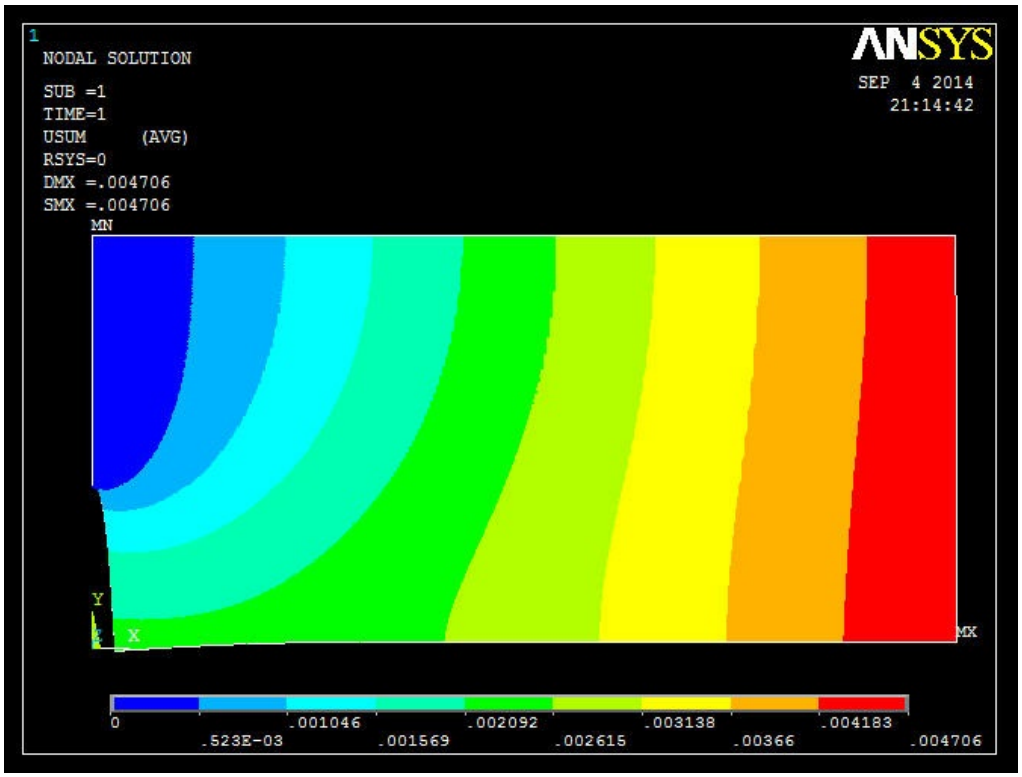

Figure 33: Deformation plot for Case 1

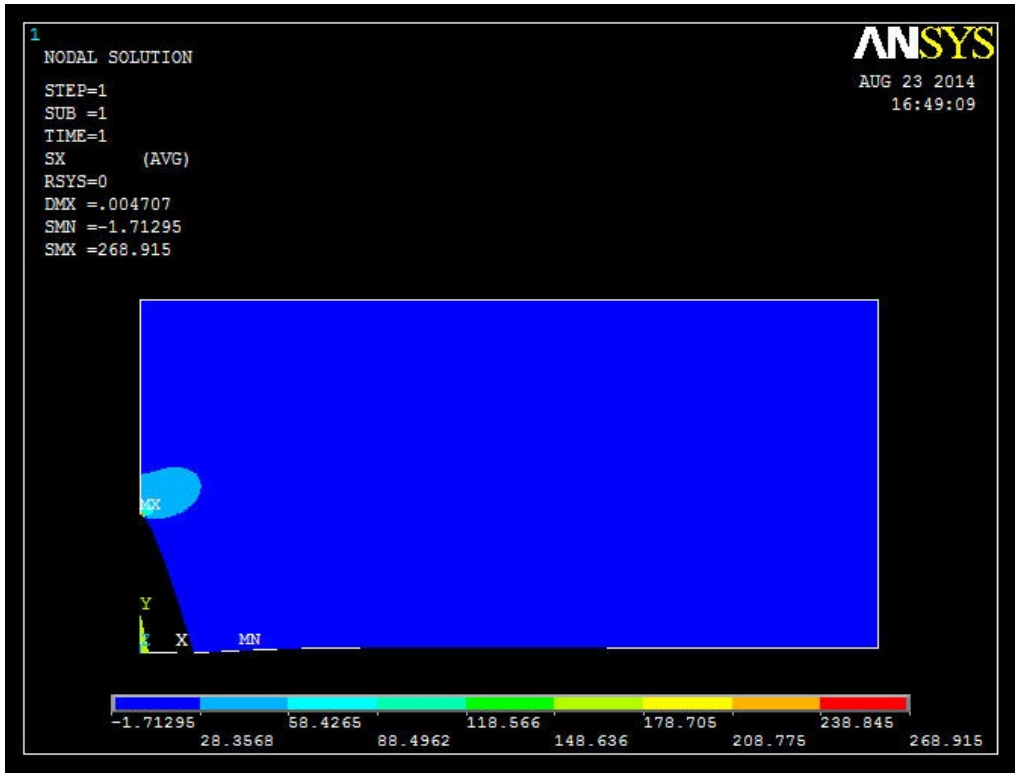

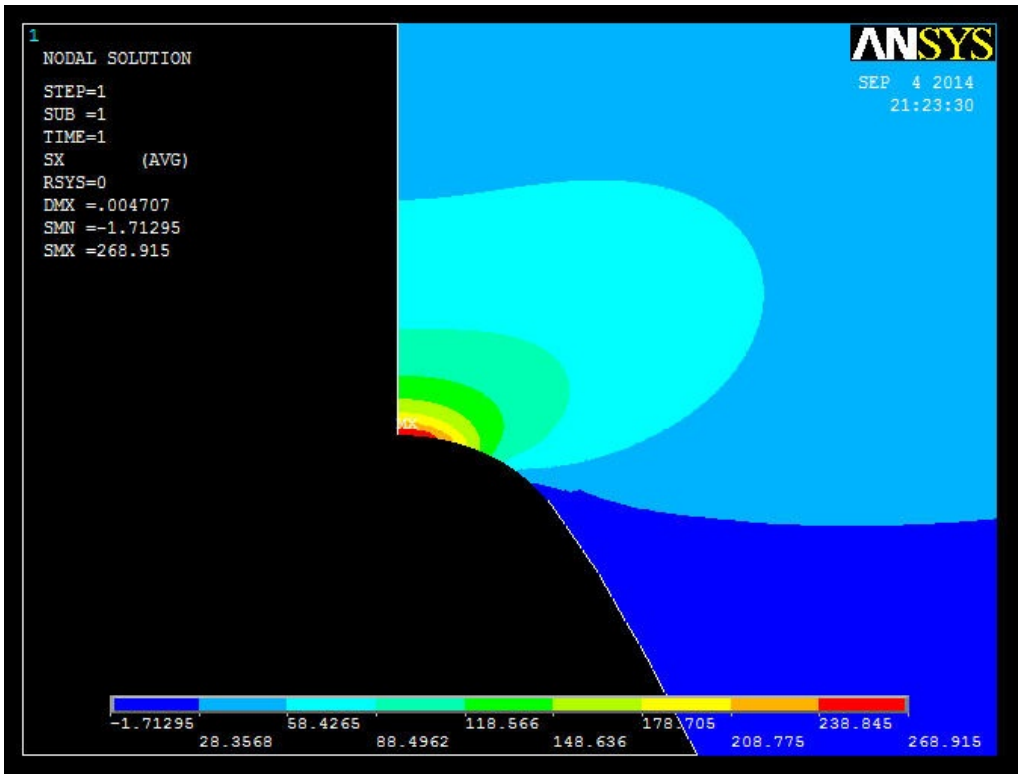

Figure 34: Stress (Sx) plot for Case 2

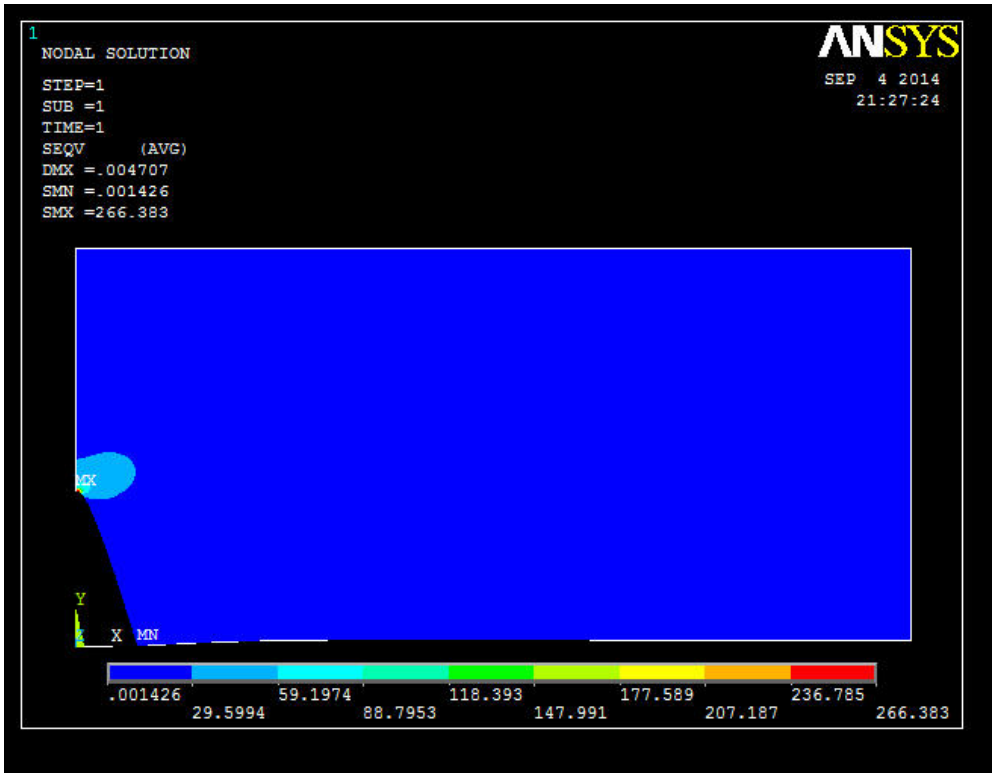

Figure 35: Von Mises Stress plot for Case 2

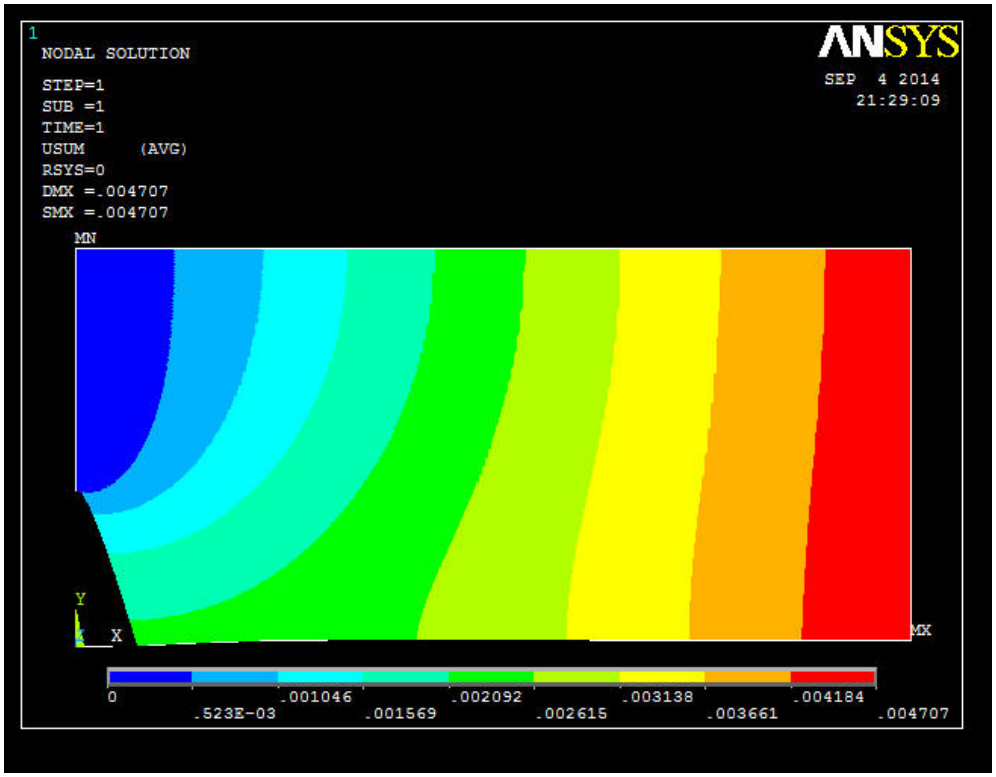

Figure 36: Deformation plot for Case 2

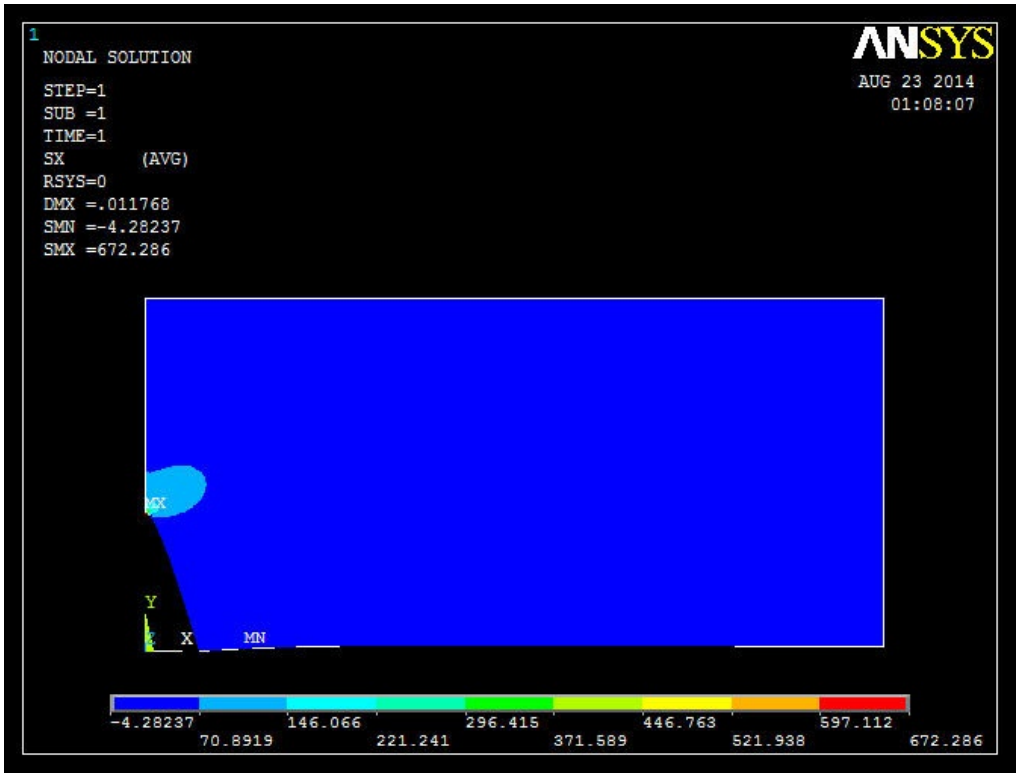

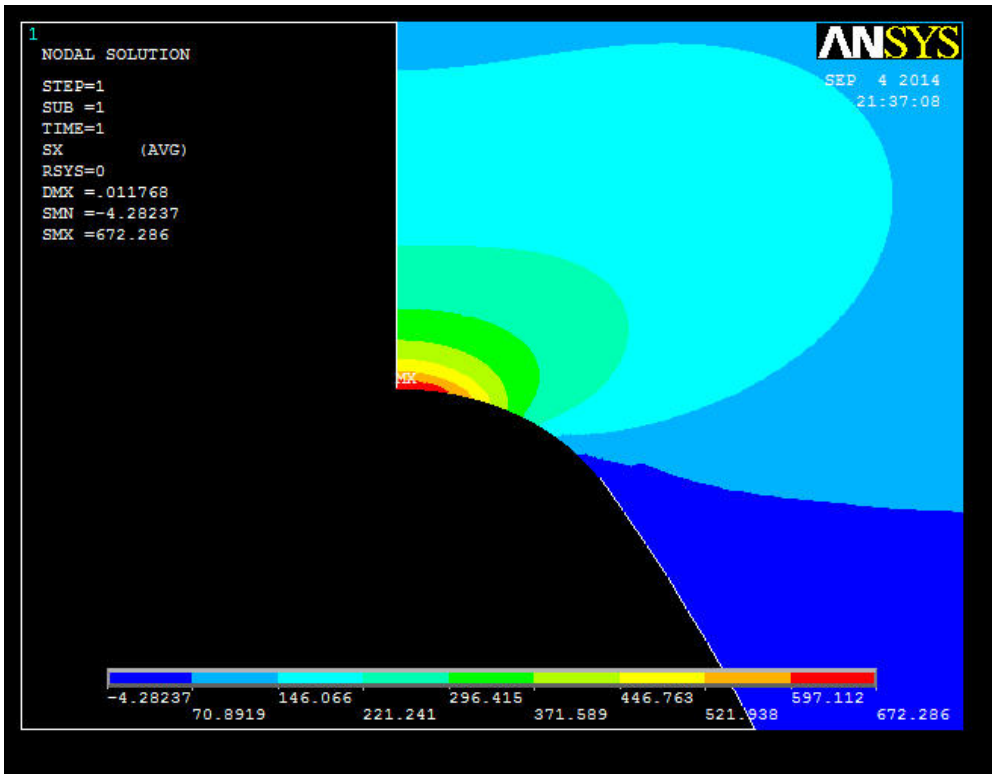

Figure 37: Stress (Sx) plot for Case 3

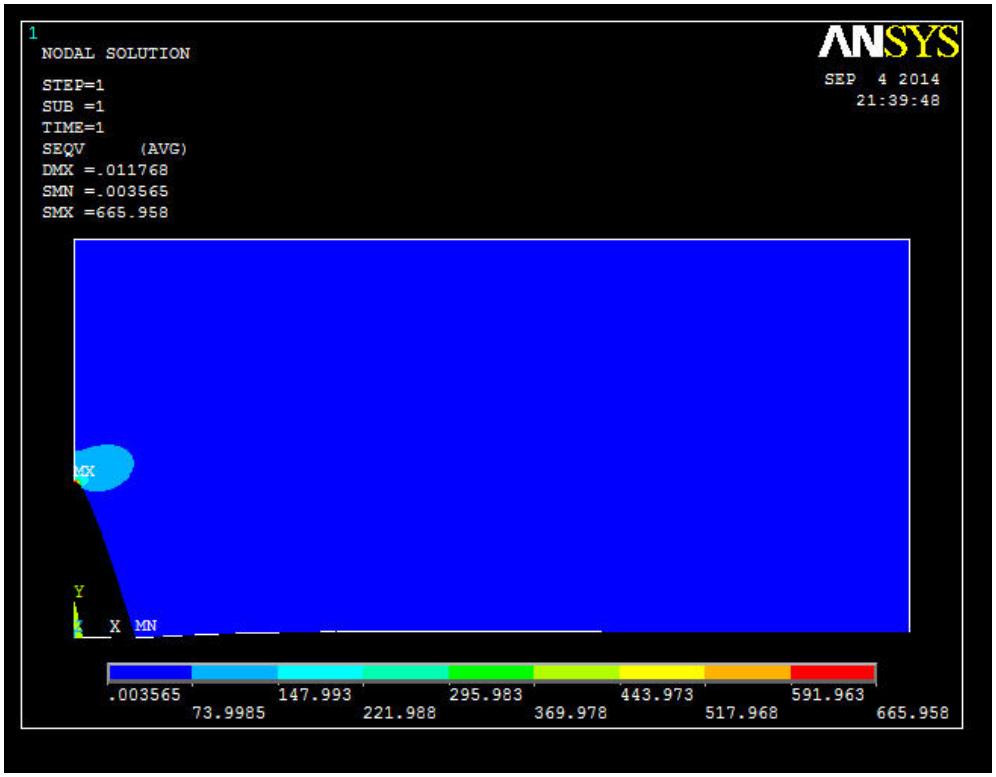

Figure 38: Von Mises stress plot for Case 3

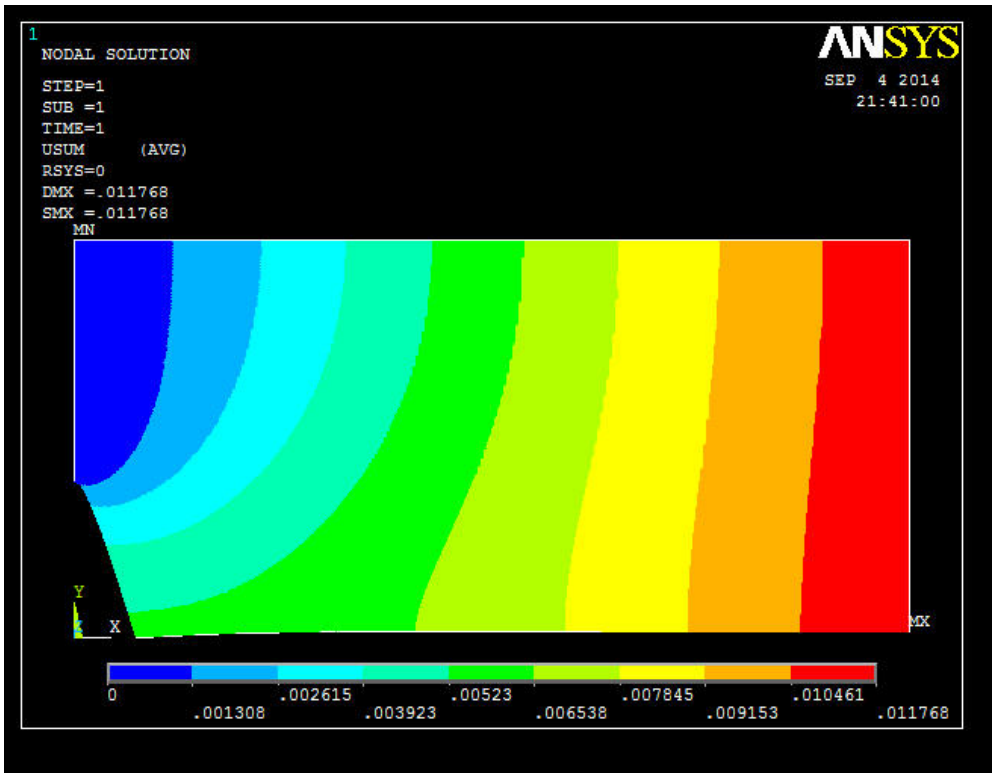

Figure 39: Deformation plot for Case 3

Appendix D - Contour plots for Stress Resolving Method

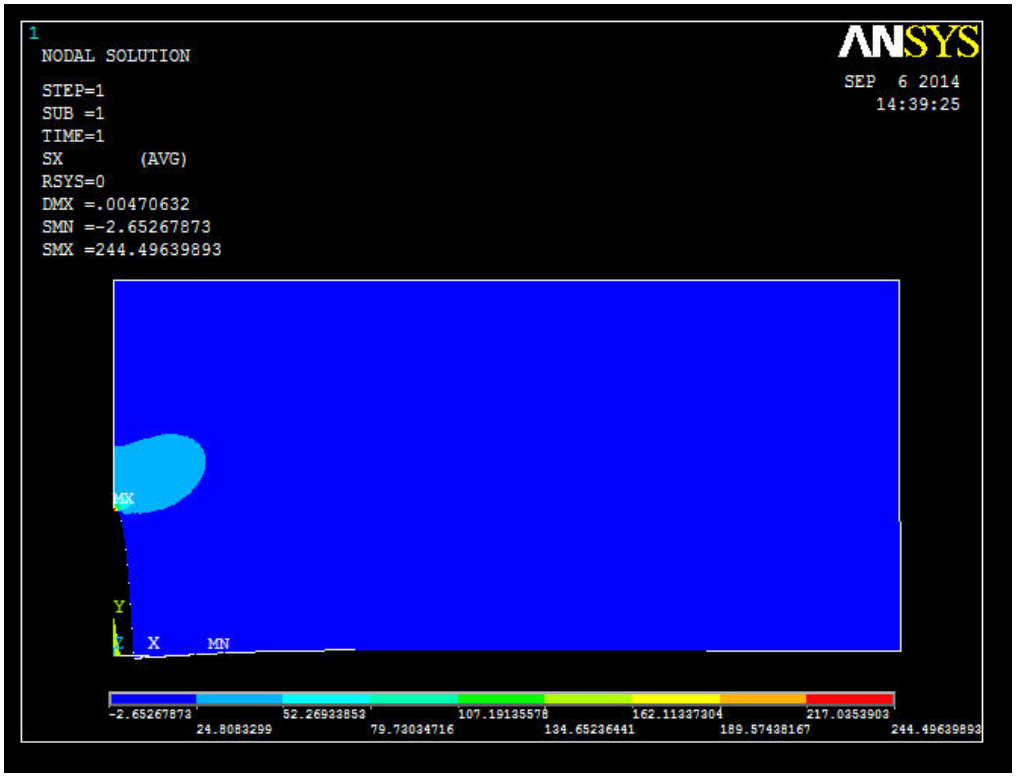

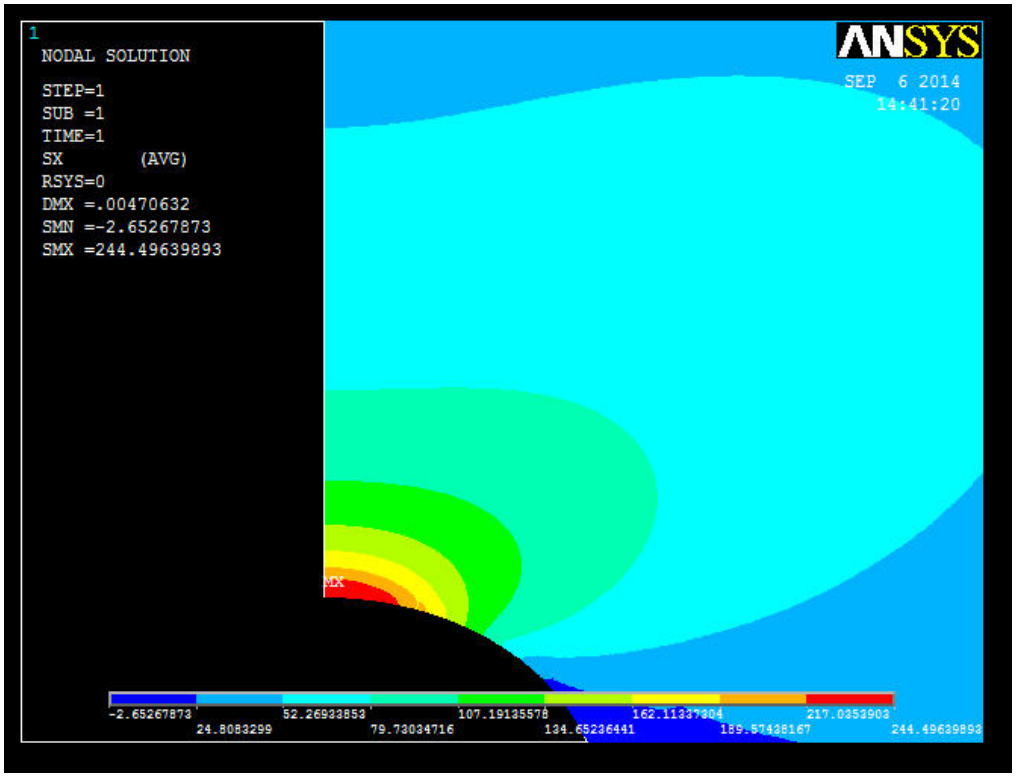

Figure 40: Stress (Sx) plot for resolved stress in Case 1

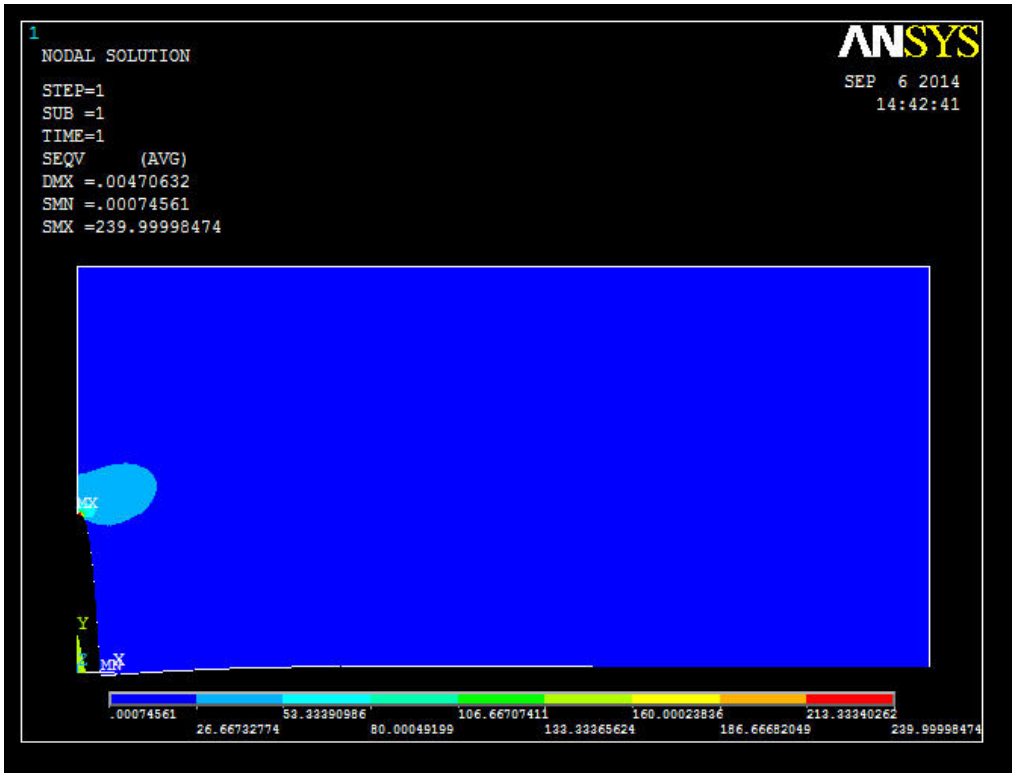

Figure 41: Von Mises plot for resolved stress in Case 1

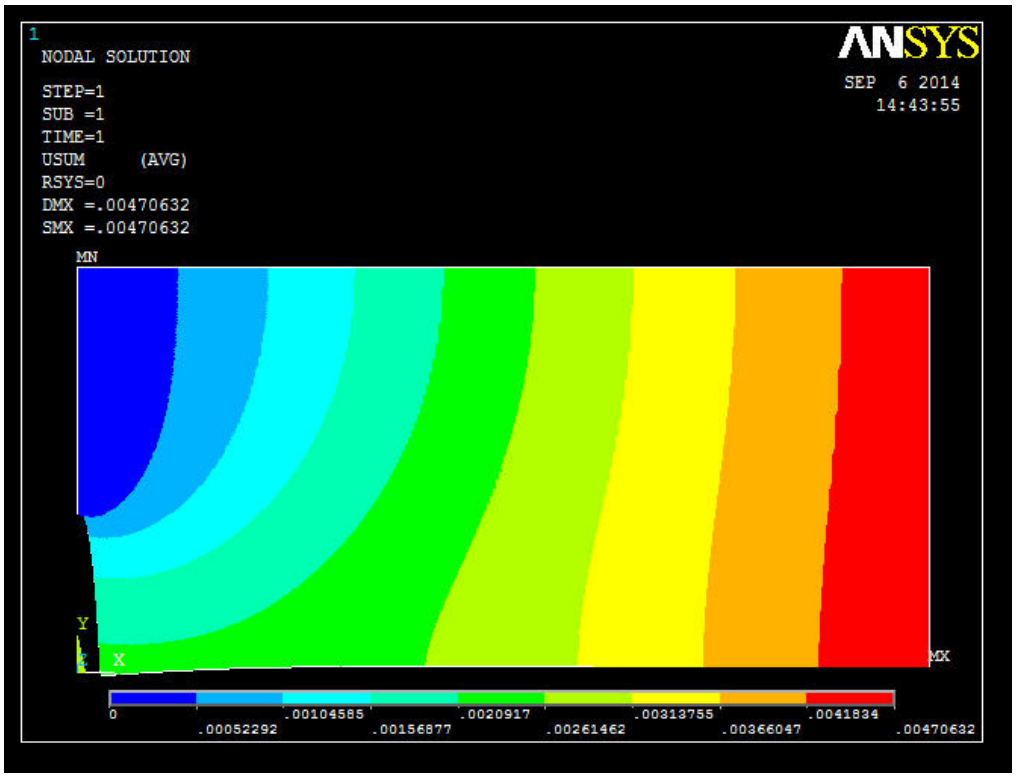

Figure 42: Deformation plot for resolved stress in Case 1

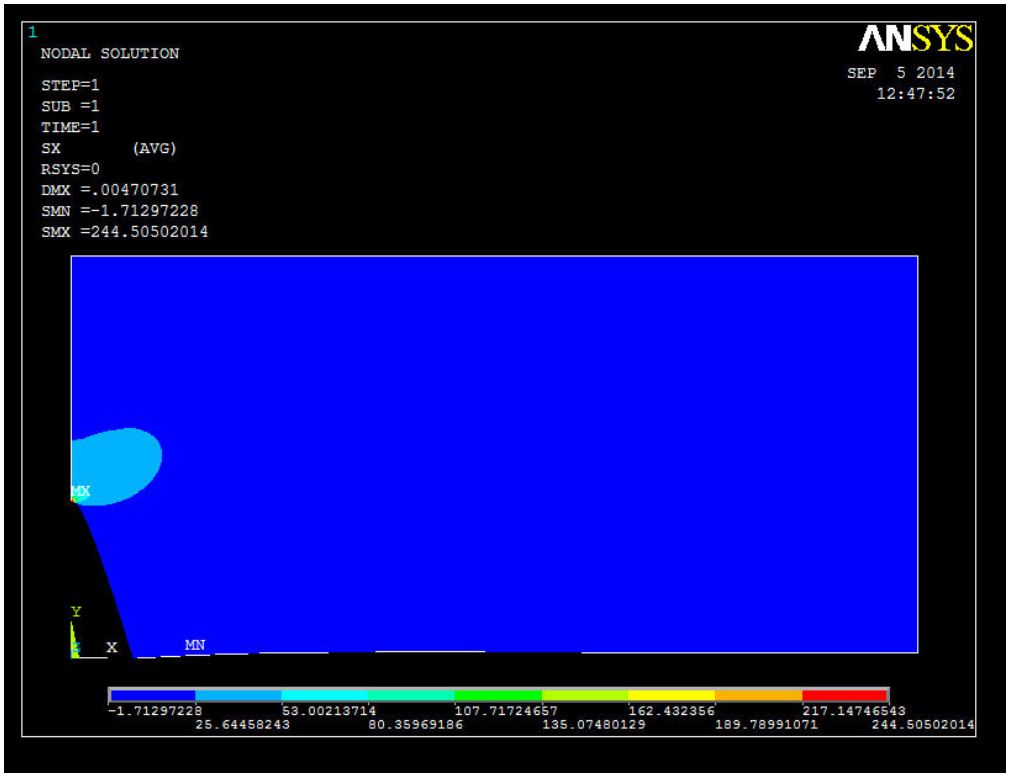

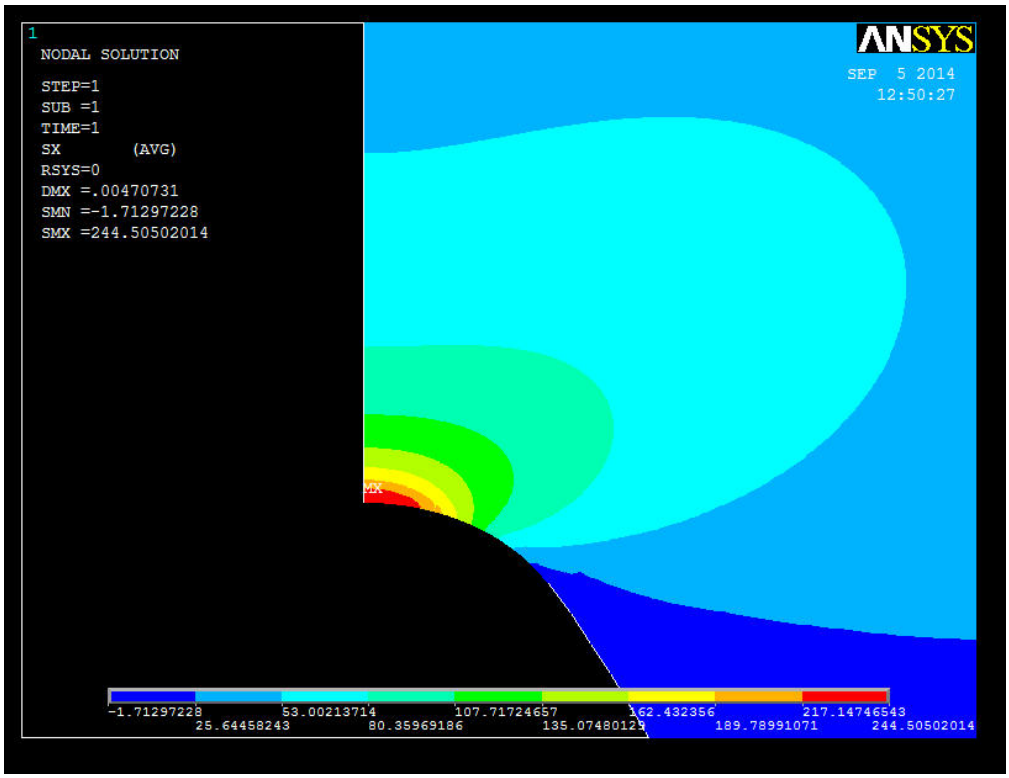

Figure 43: Stress (Sx) plot for resolved stress in Case 2

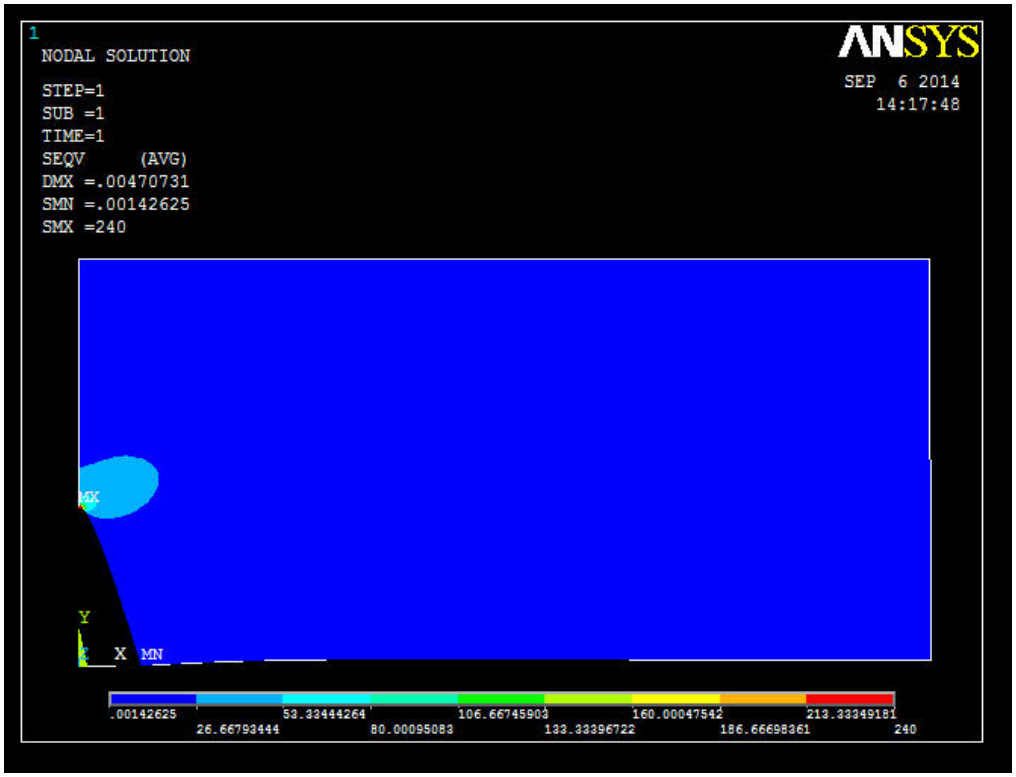

Figure 44: Von Mises plot for resolved stress in Case 2

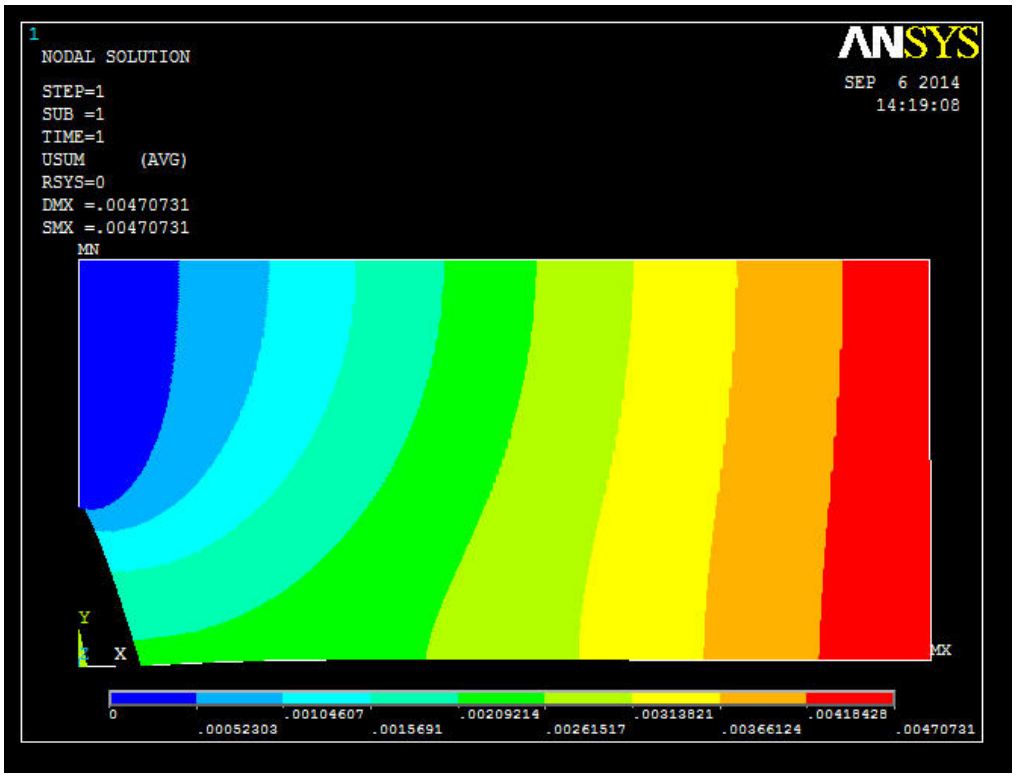

Figure 45: Deformation plot for resolved stress in Case 2

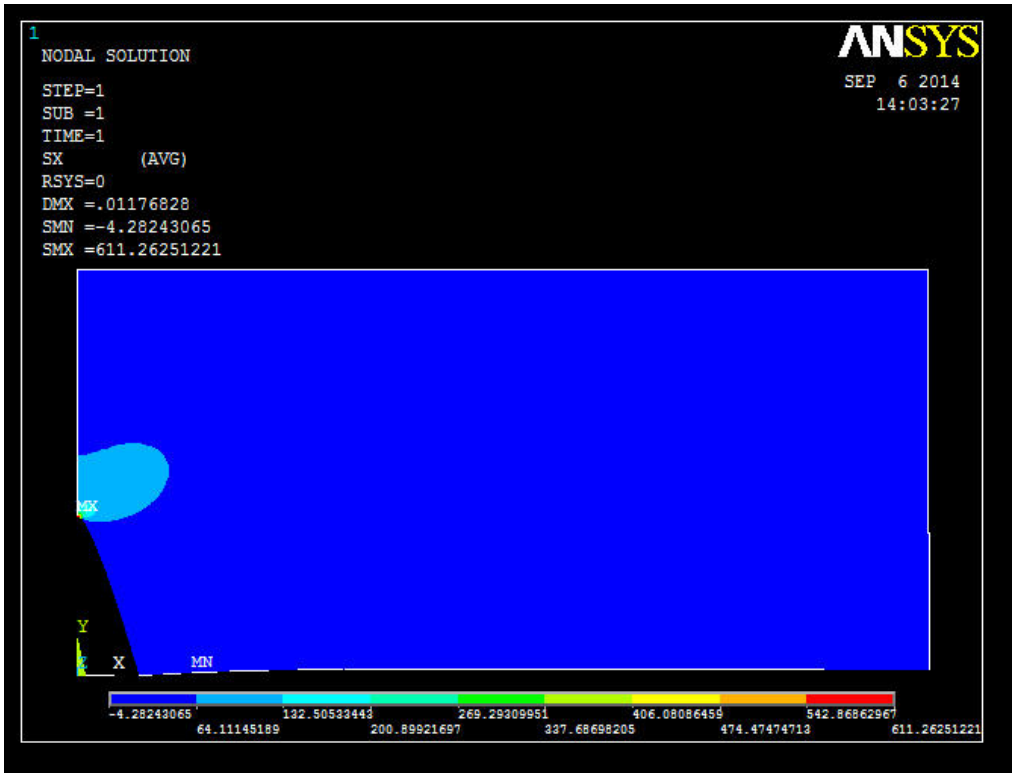

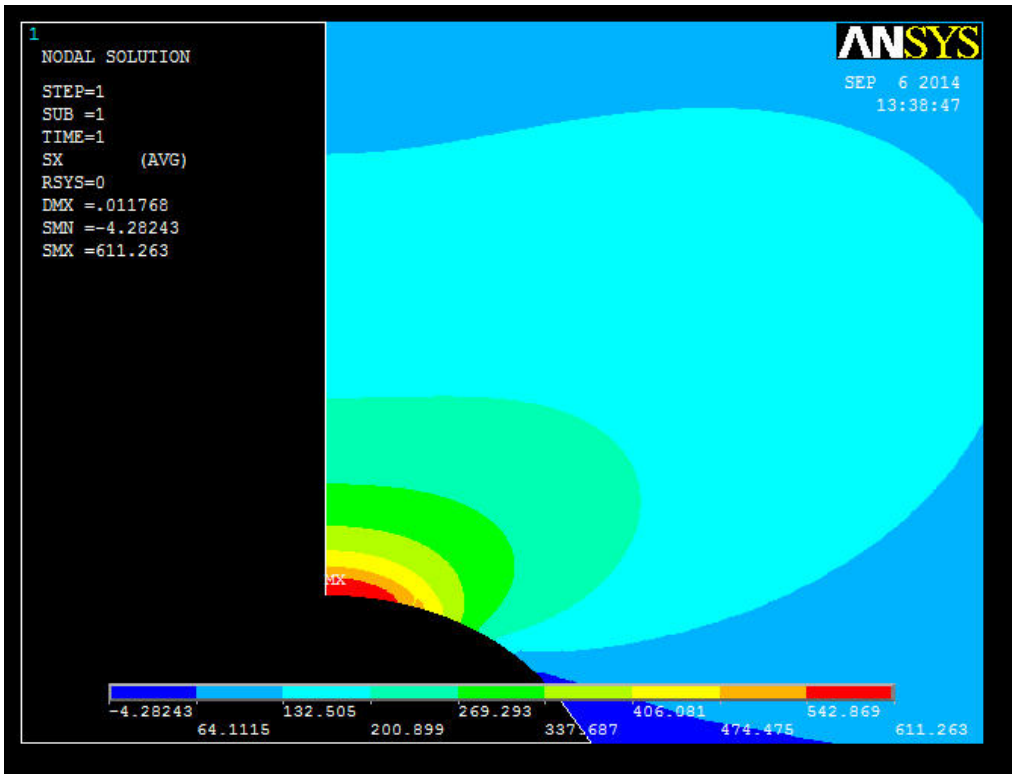

Figure 46: Stress (Sx) plot for resolved stress in Case 3

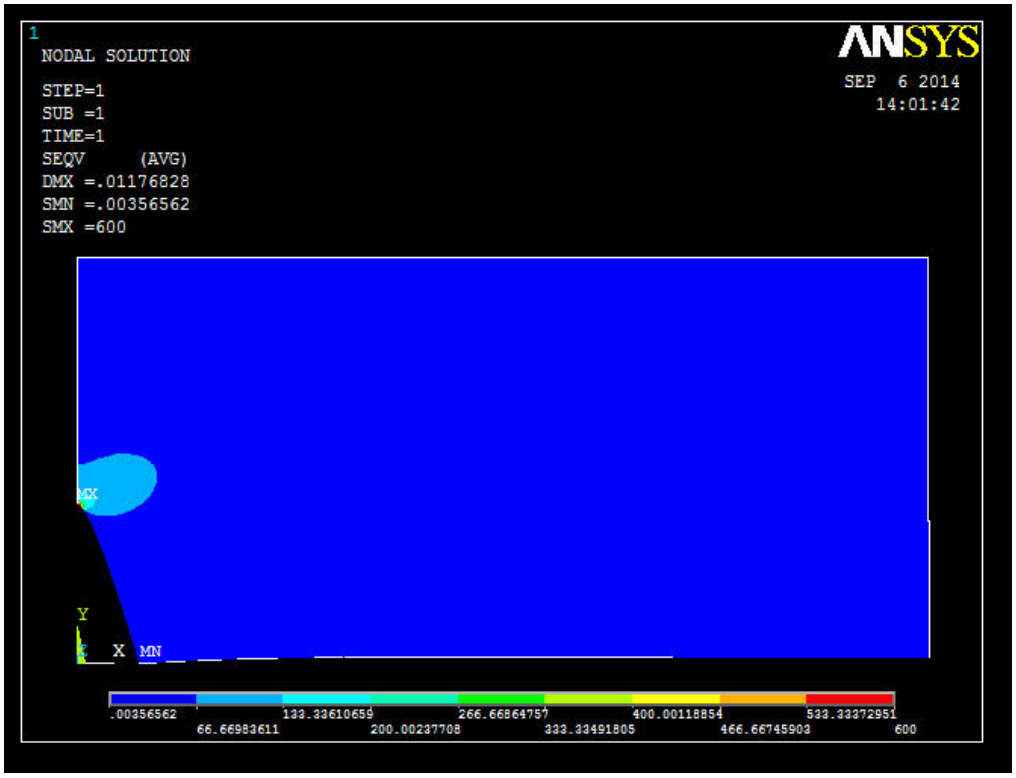

Figure 47: Von Mises plot for resolved stress in Case 3

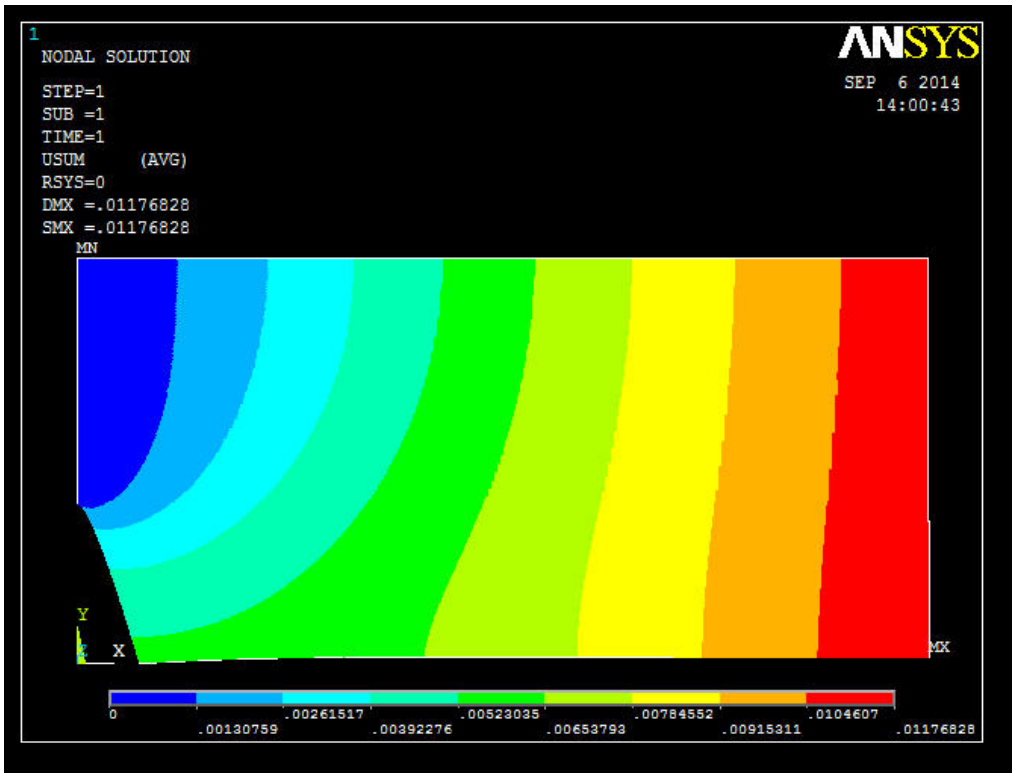

Figure 48: Deformation plot for resolved stress in Case 3